Research paper

Triterpenoid pyrazines and pyridines – Synthesis, cytotoxicity, mechanism of action, preparation of prodrugs

Jiří Hodoň [a], Ivo Frydrych [b], Zdeňka Trhlíková [a], Jan Pokorný [a], Lucie Borková [a], Sandra Benická [a], Martin Vlk [c], Barbora Lišková [b], Agáta Kubíčková [b,d], Martina Medvedíková [b], Martin Pisár [a], Jan Šarek [b], Viswanath Das [b,d], Anna Ligasová [b], Karel Koberna [b], Petr Džubák [b], Marián Hajdúch [b], Milan Urban [b,*]

[a] Department of Organic Chemistry, Faculty of Science, Palacký University Olomouc, 17. Listopadu 1192/12, 771 46, Olomouc, Czech Republic
[b] Institute of Molecular and Translational Medicine, Faculty of Medicine and Dentistry, Palacký University Olomouc, Hněvotínská 1333/5, 779 00, Olomouc, Czech Republic
[c] Czech Technical University in Prague, Faculty of Nuclear Sciences and Physical Engineering, Břehová 7, 115 19, Prague 1, Czech Republic
[d] Czech Advanced Technologies and Research Institute (CATRIN), Institute of Molecular and Translational Medicine, Palacký University Olomouc, Křížkovského 511/8, 77900, Olomouc, Czech Republic

ARTICLE INFO

ABSTRACT

A set of fifteen triterpenoid pyrazines and pyridines was prepared from parent triterpenoid 3-oxoderivatives (betulonic acid, dihydrobetulonic acid, oleanonic acid, moronic acid, ursonic acid, heterobetulonic acid, and allobetulone). Cytotoxicity of all compounds was tested in eight cancer and two non-cancer cell lines. Evaluation of the structure-activity relationships revealed that the triterpenoid core determined whether the final molecule is active or not, while the heterocycle is able to increase the activity and modulate the specificity. Five compounds (**1b**, **1c**, **2b**, **2c**, and **8**) were found to be preferentially and highly cytotoxic (IC$_{50}$ ≈ 1 μM) against leukemic cancer cell lines (CCRF-CEM, K562, CEM-DNR, or K562-TAX). Surprisingly, compounds **1c**, **2b**, and **2c** are 10-fold more active in multidrug-resistant leukemia cells (CEM-DNR and K562-TAX) than in their non-resistant analogs (CCRF-CEM and K562). Pharmacological parameters were measured for the most promising candidates and two types of prodrugs were synthesized: 1) Sugar-containing conjugates, most of which had improved cell penetration and retained high cytotoxicity in the CCRF-CEM cell line, unfortunately, they lost the selectivity against resistant cells. 2) Medoxomil derivatives, among which compounds **26–28** gained activities of IC$_{50}$ 0.026–0.043 μM against K562 cells. Compounds **1b**, **8**, **21**, **22**, **23**, and **24** were selected for the evaluation of the mechanism of action based on their highest cytotoxicity against CCRF–CEM cell line. Several experiments showed that the majority of them cause apoptosis *via* the mitochondrial pathway. Compounds **1b**, **8**, and **21** inhibit growth and disintegrate spheroid cultures of HCT116 and HeLa cells, which would be important for the treatment of solid tumors. In summary, compounds **1b**, **1c**, **2b**, **2c**, **24**, and **26–28** are highly and selectively cytotoxic against cancer cell lines and were selected for future *in vivo* tests and further development of anticancer drugs.

1. Introduction

Triterpenes are natural compounds that have various biological activities including antimalarial [1], antileishmanial [2], *anti*-HIV [3], anti-inflammatory [4], and many others [5]. Among those activities, antitumor activity is probably the most studied and important. Many research groups have been preparing semisynthetic triterpenes with high and selective cytotoxicity against cancer cells [6]. Triterpenes containing a heterocycle fused to their skeletons are one of the largest and most important classes of such compounds [7–11]. Previously, we prepared several types of heterocyclic triterpenes and among them, aminothiazoles and pyrazines prepared from betulonic acid **1a** (Fig. 1) had IC$_{50}$ in low micromolar ranges [8,11]. Two compounds are being tested *in vivo* and currently, we develop methods to uncover their

mechanism of action by finding their molecular targets [12]. Recently, another research group [9,13] published the synthesis and anti-inflammatory, antileishmanial, and other activities of heterocyclic triterpenes including pyrazine and pyridine prepared from betulonic acid **1a** that both had interesting cytotoxic activity in prostate cancer cells [14].

The main aim of this work was to investigate the cytotoxicity of triterpenoid pyridines and pyrazines and to find possible structure-activity relationships between triterpenoid 3-oxoderivatives and their corresponding pyrazines and pyridines. Seven triterpenoid oxo-compounds **1a**–**7a** (Fig. 1), representatives of five common terpenoid skeletons were chosen because their derivatives were often found to be highly cytotoxic [5]. Some of the pyrazines and pyridines are known, however, the biological activity of most of them was not described and the mechanism of action is still unknown. In this work, we expected to be able to evaluate separately the influence of each terpenic scaffold and pyridine or pyrazine ring on the cytotoxic activity. This would help us to identify the pharmacophore in each set of oxoacid–pyridine/pyrazine. In addition, pyridine and pyrazine are typical bioisosteres, therefore we expect their activities in similar ranges. Despite that, there is a number of examples in triterpenoid chemistry, where a small change in their structure (such as adding or removing one atom) may completely change bioactivities. Hemiesters of betulinic acid are one of the examples in which a small change at the hemiester moiety causes a large change in the activity against HIV [16]. The second example may be 2,2-difluoroderivatives of betulinic acid where replacement of hydrogens at C-2 with supposedly bioisosteric fluorine atoms yielded products with significantly higher cytotoxicity and lower selectivity than the parent betulinic acid [17]. Therefore, we also focused on pointing on the influence of the presence/absence of one aromatic nitrogen on the activity.

In the first part of the study, we used all compounds as free carboxylic acids unprotected because it is known that in most triterpenoid acids, compounds containing the free 28-carboxylic group are more cytotoxic than their esters [18,19]. Later, we used 28-carboxyl for the introduction of potential prodrug moiety. All compounds were tested on eight cancer cell lines including multidrug resistant phenotypes, and on two non-cancer fibroblast lines.

2. Results and discussion

2.1. Chemistry

2.1.1. Synthesis of basic heterocyclic triterpenoids

The synthesis of pyrazines **1b**–**7b** (Scheme 1 and Fig. 2) was described in Refs. [8,15] and the synthesis of pyridine **1c** (Fig. 2) is described in Refs. [9,13] with a rather low yield of 12% (Scheme 1).

Most of the published compounds were not tested on any biological activity and therefore we resynthesized them and tested as a part of this study. Compounds **2c**–**7c** (Fig. 2) are new. Our first goal was to optimize the procedure for the synthesis of pyridines by extending the reaction time and varying the amount of the catalyst. Unfortunately, this only allowed increasing of the yield to 23–35% for derivatives **1c**, **2c**, **3c**, **5c**, and **7c**, while for compounds **4c** and **6c** yield was still below 10%. Another improvement was adding an activated molecular sieve to the reaction mixture, which allowed for 48% of **6c** but still only 15% of **4c**. Therefore, we changed the CuCl catalyst for more reactive NaAuCl$_4$·2H$_2$O and obtained 41% of **4c**. Within those optimization experiments, all target derivatives were prepared in sufficient amounts for full characterization and all extensive biological tests; therefore, we discontinued further seek for higher yields. We also oxidized pyrazine **1b** using SeO$_2$ which gave 30-oxoderivative **8** (Scheme 1) and included this compound in our study. It is known that 30-oxobetulinic acid **11**
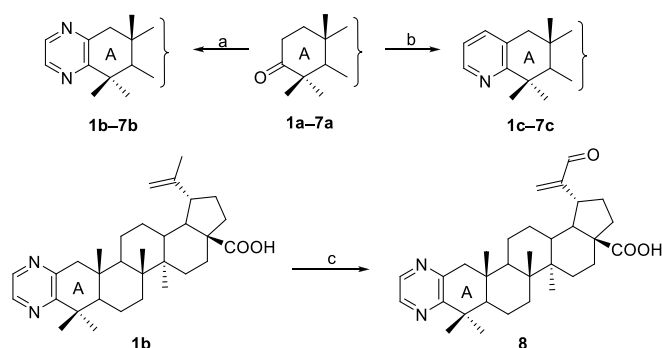
Scheme 1. Preparation of triterpenoid pyrazines and pyridines. Reagents and conditions: a) ethylenediamine, sulfur, morpholine, reflux; b) propargylamine, CuCl, ethanol, reflux or propargylamine, NaAuCl$_4$·2H$_2$O, ethanol, reflux; c) SeO$_2$, 2-methoxyethanol, reflux.
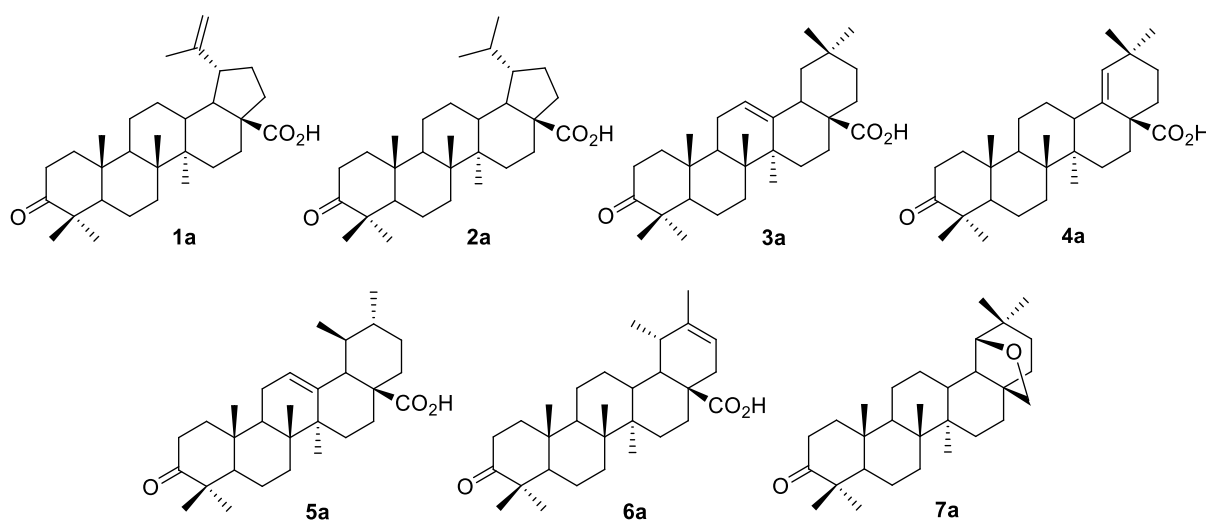

Fig. 1. Starting 3-oxotriterpenes – betulonic acid **1a**, dihydrobetulonic acid **2a**, oleanonic acid **3a**, moronic acid **4a**, ursonic acid **5a**, heterobetulonic acid **6a**, and allobetulon **7a**.
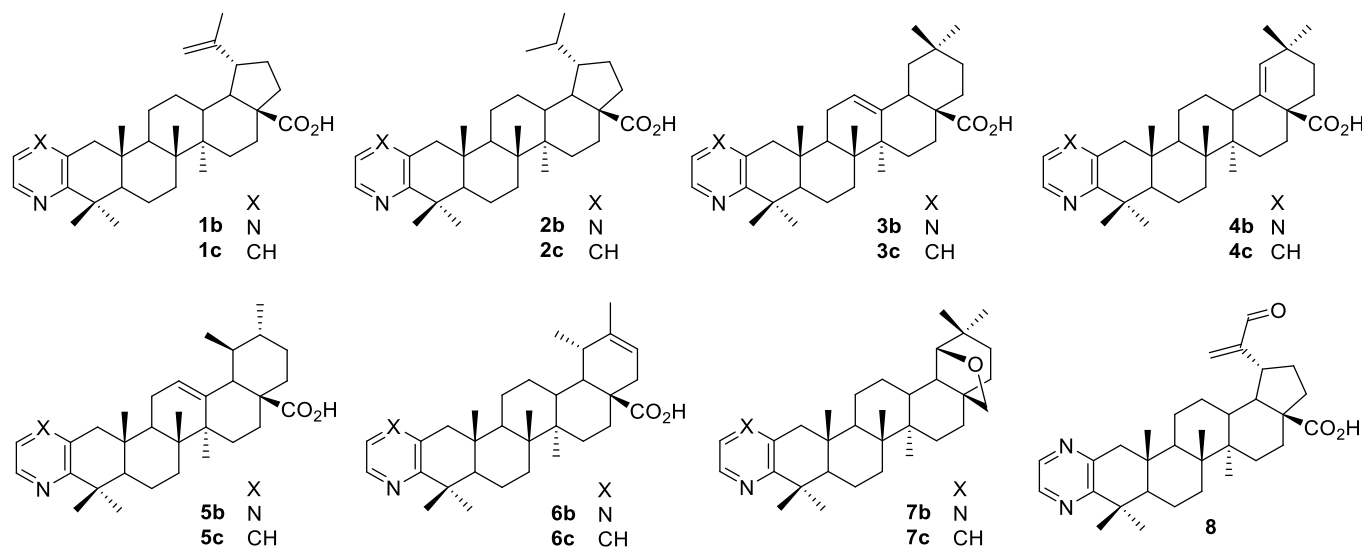
Fig. 2. Triterpenoid pyrazines **1b**–**7b**, pyridines **1c**–**7c**, and pyrazine **8**.

(Scheme 3) is more soluble in water than betulinic acid **9**, and in addition, compound **11** has high cytotoxic activity [20]. For these reasons, we included both 30-oxoderivatives **8** and **11** in this study.

2.1.2. Synthesis of prodrugs

Two sets of prodrugs were prepared within this study – glucose conjugates **15**–**22** (Schemes 2 and 3) and medoxomil derivatives **23**–**28** (Scheme 4). Synthesis of both sets was motivated by the preliminary results from the biological screening and by the literature, sugar-containing triterpenes prepared earlier in our research group had high activity and bioavailability in *vivo* murine experiments [21] and medoxomil is known to increase the bioavailability of ursolic acid *in vivo* [22]. Glucose derivatives were prepared from betulinic acid **9**, 30-oxoderivatives **8** and **11**, and pyrazine **1b** in order to compare the influence of the glucose part on pharmacological parameters and on the cytotoxic activity.

Glucose conjugates **15**–**22** were prepared *via* a Cu-mediated azide-alkyne cycloaddition of corresponding terpenic propargyl esters (**10**, **12**, **13**, and **14**), and 2,3,4,6-tetra-O-acetyl-β-ᴅ-glucopyranosyl azide **II** or β-ᴅ-glucopyranosyl azide **III** (Schemes 2 and 3) using a similar procedure as in Ref. [25]. The first attempts, using CuI at room temperature, were unsatisfactory because of low yields (10–15%). Raising the temperature to 40 °C with the same catalyst allowed to increase the yields by 35%–54%. These lower yields were mostly caused by repeated semi-preparative HPLC in order to ensure the highest possible purity for biological tests.

Medoxomil derivatives **23**–**28** were prepared by the alkylation of the free carboxylic acids **9**, **1a**, **1b**, **1c**, **2b**, and **2c** with 4-chlorometyl-5-metyl-1,3-dioxolone in the presence of KI and K_2CO_3 in acetone [22]. The reactions with medoxomil were terminated after 24 h at room temperature with yields of 74–96%.
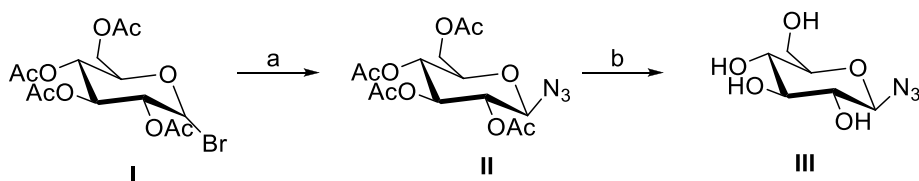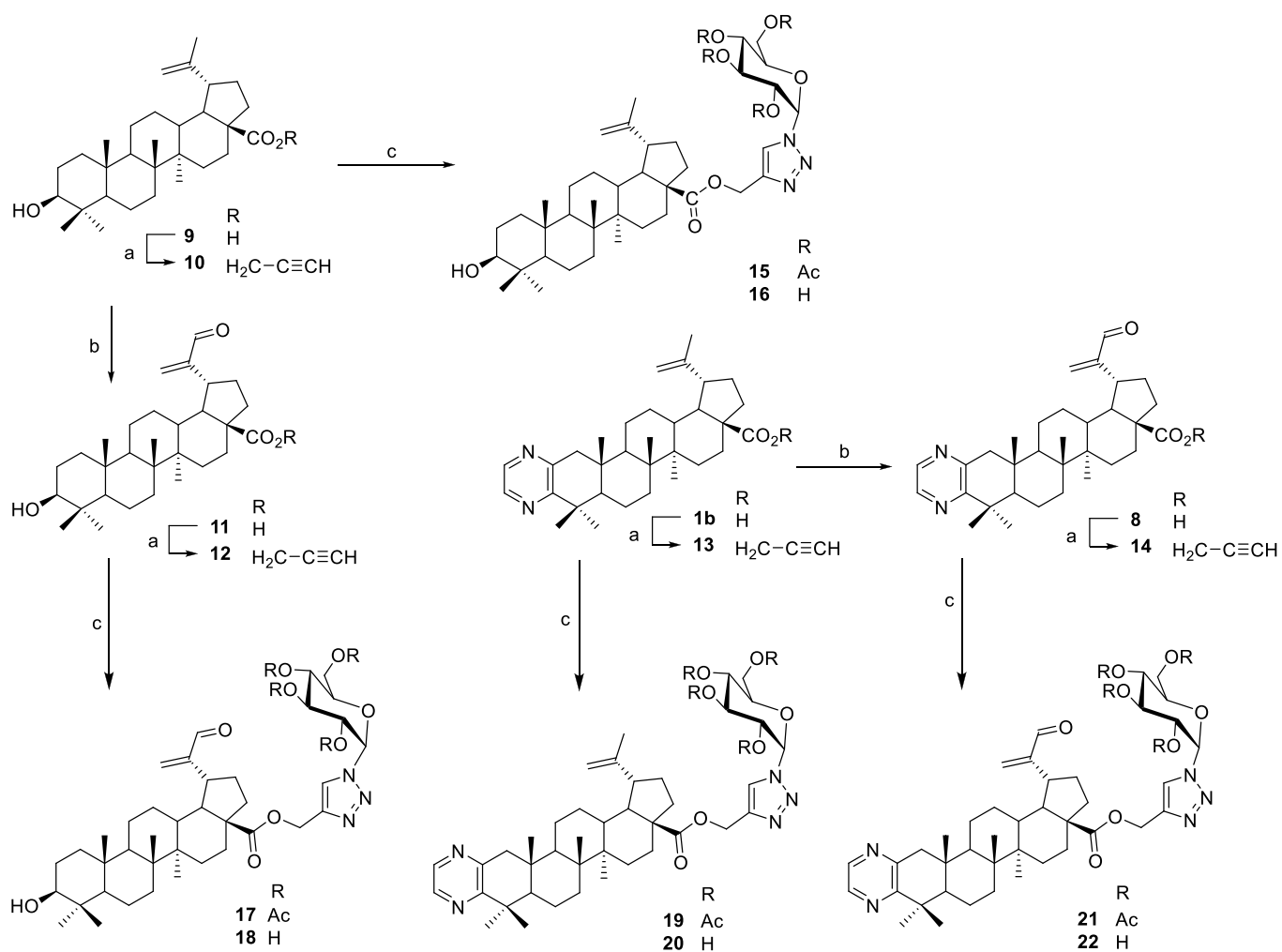
2.2. Biology

2.2.1. Cytotoxicity assay

Cytotoxic activity of all prepared compounds was tested on eight cancer cell lines and two non-cancer fibroblasts (Table 1). From various triterpenic skeletons, both pyrazine and pyridine derivatives of lupane (**1b**, **1c**, **2b**, **2c**, and **8**) and taraxastane (**6b** and **6c**) were found to be the most active (IC_{50} = 0.52–8.0 μM) and most promising for further development. Oleanane, ursane, and 18α-oleanane heterocycles (**3b**, **3c**, **4b**, **4c**, **5b**, **5c**, **7b**, and **7c**) had the IC_{50} above 10 μM and they were not further evaluated as the potential anticancer drug candidates. Pyrazine **1b** had the IC_{50} 0.53 μM in CCRF-CEM cell line and importantly, it had a very high TI = therapeutic index (higher than 94) since its IC_{50} in healthy fibroblast cells was above 50 μM. Pyrazine **8** containing an aldehyde in position C-30 was highly cytotoxic, however, its selectivity (TI = 3.6) was insufficient and analogous pyridine derivative was not synthesized. Despite that, molecule **8** was included in further development since the introduction of a prodrug moiety could change this lack of selectivity.

An important discovery among pyridine and pyrazine derivatives **1b**, **1c**, **2b**, and **2c** is their activity against drug-resistant leukemic cell lines CEM-DNR and K562-TAX. Compound **1b** has almost the same high activity in CCRF-CEM cells and CEM-DNR cells (IC_{50} = 0.53 and 0.63 μM) and lower activity in K562 and K562-TAX cells (IC_{50} = 11.5 and 11.6 μM). Surprisingly, pyrazine **2b** has about 20-fold higher activity against resistant CEM-DNR cells (IC_{50} = 0.52 μM) than against non-resistant CCRF-CEM cells (IC_{50} = 10 μM) and the activity against the resistant K562-TAX (IC_{50} = 0.52 μM) is 35-fold higher than in nonresistant K-562 cells (IC_{50} = 18 μM). Pyridines **1c** and **2c** have low activity in CCRF-CEM cells (IC_{50} is more than 20 μM) and high activity in CEM-DNR cells (IC_{50} is 2.4 and 2.0 μM). Similarly, the activity of **1c** and **2c** in resistant leukemic cells K562-TAX (IC_{50} is 1.9 and 1.4 μM) is about 10-fold higher

Scheme 2. Synthesis of 2,3,4,6-tetra-O-acetyl-β-ᴅ-glucopyranosyl azide **II** and β-ᴅ-glucopyranosyl azide **III** according to the lit [23,24]. Reagents and conditions: a) NaN₃, EtOH, r.t.; b) EtONa, EtOH, r.t.

Scheme 3. Preparation of triterpenoid conjugates with glucose. Reagents and conditions: a) propargyl bromide, K$_2$CO$_3$, DMF, r.t.; b) SeO$_2$, 2-methoxyethanol, reflux (ref. [26]); c) **II** or **III**, CuI, DMF, 40 °C.
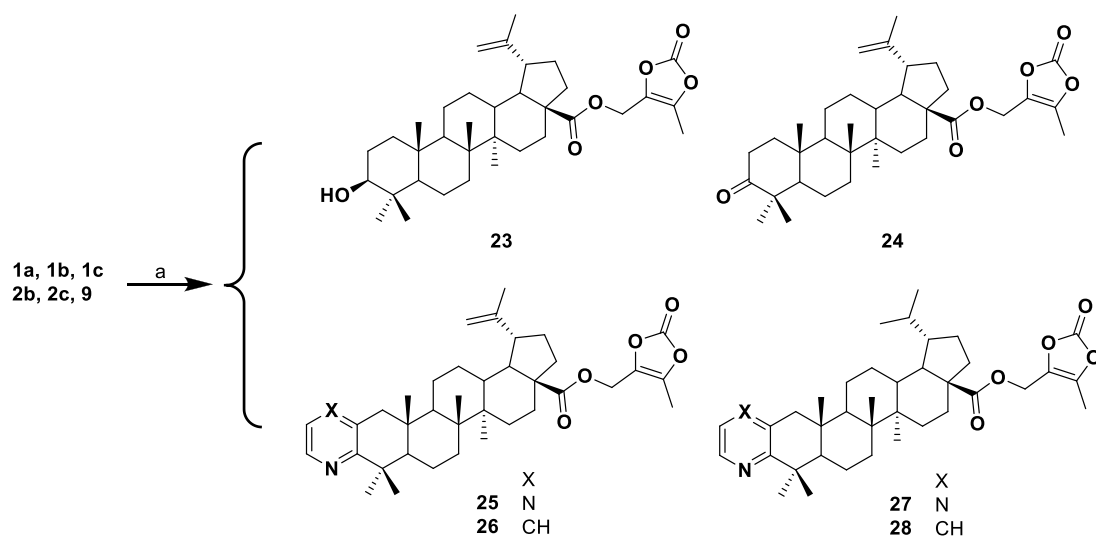
Scheme 4. Synthesis of medoxomil prodrugs **23**–**28**. Reagents and conditions: a) 4-(chloromethyl)-5-methyl-1,3-dioxol-2-one, KI, K$_2$CO$_3$, acetone, r.t.

Table 1
Cytotoxic activities of tested compounds on eight tumor (including multidrug resistant) and two normal fibroblast cell lines.

Comp.	IC$_{50}$ (µM/L)[a]										TI[b]
	CCRF-CEM	CEM-DNR	K562	K562-TAX	HCT116	HCT116p53$^{-/-}$	A549	U2OS	BJ	MRC-5	
1a	8.4	11	14	15	38	49	40	38	39	30	4.1
1b	0.53	0.63	12	12	34	47	32	32	>50	>50	>94
1c	23	2.4	13	1.9	35	>50	27	>50	>50	>50	>2.2
2a	6.3	48	12	11	34	36	22	27	>50	>50	>8.0
2b	10	0.52	18	0.52	22	23	21	29	>50	>50	>4.9
2c	22	2.0	11	1.4	31	>50	46	>50	>50	>50	>2.3
3a	9.5	17	>50	21	45	>50	50	49	>50	>50	>5.2
3b	18	14	>50	34	50	>50	50	>50	>50	>50	>2.8
3c	39	>50	13	>50	>50	>50	>50	>50	>50	>50	>1.3
4a	17	17	>50	21	45	>50	47	>50	>50	>50	>2.9
4b	15	29	>50	25	40	>50	>50	>50	>50	>50	>3.4
4c	8.0	14	>50	15	47	>50	>50	>50	>50	>50	>6.2
5a	16	19	>50	27	47	>50	50	>50	>50	>50	>3.1
5b	19	17	>50	44	50	>50	>50	>50	>50	>50	>2.7
5c	38	40	32	47	>50	>50	>50	>50	>50	>50	>1.3
6a	6.5	11	8.5	28	32	35	24	24	35	33	5.2
6b	7.2	10	18	10	48	50	44	46	>50	>50	>7.0
6c	6.3	11	12	13	34	34	20	35	>50	>50	>8.0
7a	>50	>50	>50	>50	>50	>50	>50	>50	>50	>50	–
7b	>50	>50	>50	>50	>50	>50	>50	>50	>50	>50	–
7c	>50	>50	>50	>50	>50	>50	>50	>50	>50	>50	–
8	0.67	2.1	2.3	0.86	2.0	2.1	3.9	2.7	3.0	1.8	3.6

[a] The concentration of drug needed to inhibit cell growth by 50%. The standard deviation in cytotoxicity assays is typically up to 15% of the average value.
[b] Therapeutic index is calculated for IC$_{50}$ of CCRF-CEM line vs average of both fibroblasts.

than in non-resistant cells K562 (IC$_{50}$ is 13.4 and 10.5 µM). We found it really interesting, that such a small isosteric exchange (replacement of aromatic nitrogen with C–H and saturation of a double bond) in a triterpenoid molecule can induce such a large impact on the activity and this should be subject of more future studies. As a part of the development of the most active compounds **1b**, **1c**, **2b**, **2c**, and **8**, we measured their ADME parameters and tried to adjust the lipophilicity of the molecule **1b** by synthesizing prodrugs **15–22** (*via* propargyl ester precursors **10**, **12**, and **14**) in order to improve its bioavailability. Compound **1b** was selected as a representative for all active compounds, it was expected that the influence of prodrug moiety on all active compounds is similar. In addition, we prepared medoxomil conjugates **23–28** from the starting acids **1a** and **9** and from the most interesting compounds **1b**, **1c**, **2b**, **2c**. The *in vitro* cytotoxic activity of compounds **10–28** is summarized in Table 2. First of all, 30-oxoderivatives **12**, **17**, and **21** are active (IC$_{50}$ in all cancer cell lines 0.6–2.7 µM) but they

remained unselective (TI 2.8–5.0). In contrast, 30-oxoderivatives **14**, **18**, and **22** remained active in CCRF-CEM cell line (IC$_{50}$ 0.43–4.6 µM) and gained selectivity, since they are less cytotoxic in both fibroblast lines but also in several cancer cell lines (TI > 10). Conjugates **15**, **16**, **19**, **20** (betulinic acid **9** and pyrazine **1b** connected with glucose) had activity in higher micromolar concentration ranges. The most significant improvement of the activity was achieved among medoxomil derivatives **23–28**. It was found that compounds **23**, **24**, and **25** are active in CCRF-CEM cell line with sufficient selectivity. Compounds **24**, and **26–28** are significantly active against the second leukemia cell line K562 with IC$_{50}$ between 0.037 and 0.87 µM and their selectivity is also high. Concerning cytotoxicity across the entire panel of cancer cell lines used, compounds **26–28** are to date the most active triterpenes prepared in our lab. Since the medoxomil part is supposed to be metabolized *in vivo* to obtain an active parent compound [22], we did not measure their ADME parameters. Compounds **23–28** will be included in the future *in*

Table 2
Cytotoxic activities of prodrugs on eight tumor (including multidrug-resistant) and two normal fibroblast cell lines.

Comp.	IC$_{50}$ (µM/L)[a]										TI[b]
	CCRF-CEM	CEM-DNR	K562	K562-TAX	HCT116	HCT116p53$^{-/-}$	A549	U2OS	BJ	MRC-5	
10	24	40	43	36	33	31	43	31	32	26	1.2
12	0.88	1.4	1.8	1.3	1.7	1.5	1.3	1.6	7.1	1.7	5
13	45	50	>50	>50	>50	>50	>50	>50	>50	>50	>1.1
14	0.43	1.7	1.6	1.4	7.0	6.3	1.7	1.4	7.2	6.6	16
15	>50	>50	>50	>50	>50	>50	>50	>50	>50	>50	–
16	>50	>50	>50	>50	>50	>50	>50	>50	>50	>50	–
17	0.60	1.6	1.4	1.6	1.6	1.7	1.8	1.7	1.8	1.7	2.9
18	4.6	>50	21	>50	38	41	>50	50	>50	>50	11
19	>50	49	>50	>50	>50	>50	>50	>50	>50	>50	–
20	8.1	19	19	21	30	28	38	20	42	>50	5.7
21	0.75	1.5	1.2	2.7	1.5	1.7	1.8	1.6	2.3	1.8	2.8
22	2.0	>50	5.2	46	7.2	7.8	28	8.2	26	28	14
23	4.5	14	8.3	12	17	15	13	19	44	41	9.4
24	2.3	9.1	0.87	11	21	19	9.5	22	>50	47	>21
25	3.6	0.49	>50	13	40	49	10	45	>50	>50	14
26	35	48	0.037	49	>50	>50	50	>50	>50	>50	>1.4
27	17	50	0.026	12	>50	44	41	40	>50	>50	2.9
28	46	50	0.043	>50	>50	>50	>50	>50	>50	>50	>1.1

[a] The concentration of drug needed to inhibit cell growth by 50%. The standard deviation in cytotoxicity assays is typically up to 15% of the average value.
[b] Therapeutic index is calculated for IC$_{50}$ of CCRF-CEM line vs average of both fibroblasts.

vivo tests to determine their behavior in living organisms and to show if it is worth to use this prodrug moiety. Finally, based on above-mentioned findings, we decided to select the most cytotoxic compounds on sensitive CCRF-CEM cells among pyridine and pyrazine derivatives (**1b** and **8**) and their prodrugs (**21**–**24**) and subject them for advanced biological experiments to evaluate their mechanism of action.

2.2.2. Pharmacological parameters

In order to pass the most active compounds **1b**, **1c**, **2b**, **2c**, and **8** further into our drug discovery program, we measured their *in vitro* ADME parameters that are summarized in the Table 3. Tested compounds demonstrated quite a high chemical stability in phosphate-buffered saline (PBS pH 7.4) after 120 min at 37 °C. Also, all compounds were found to be stable in plasma (all compounds showed more than 85% presence in plasma after 120 min). The intrinsic clearance data obtained in microsomal stability assay showed low or medium category. This means that all studied compounds were not subject to rapid metabolism by liver microsome enzymes. All five derivatives **1b**, **1c**, **2b**, **2c**, and **8** had the low ability (- log Papp >6 cm/s) to diffuse passively through an artificial cellular membrane in the Parallel artificial membrane permeability assay (PAMPA), suggesting an alternative intracellular transport mechanism. The MDCK-MDR1 permeability assays are established models of blood-brain barriers [27]. Studied compounds showed a low ability to cross the blood-brain barrier. All derivatives were not actively exported from the cells in a barrier model as indicated by efflux ratios <2. To conclude, the first set of the molecules **1b**, **1c**, **2b**, **2c**, and **8** had excellent chemical, plasma, and microsomal stability, however, it was necessary to consider which structural changes could achieve better cell permeability.

Compounds **1b** and **8** were selected as model examples for conjugation with glucose analogs in order to optimize their properties. Similar conjugates were prepared from betulinic acid **9** and aldehyde **11** to obtain more information about the structure-property relationships in this set of compounds. The main goal was to select the best modifying moiety to be able to use it in the future to improve the properties of the final candidate. As a result, a set of derivatives **15**–**22** was prepared and the ADME parameters are shown in the Table 4. The conjugates **15**–**22**

showed good stability parameters, we observed more than 80% presence in plasma after 120 min and low or medium category of intrinsic clearance using microsomal stability assay. It is important because the instability in plasma and liver microsomes can result in rapid clearance, short half-life, and poor *in vivo* performance. Conjugates **19** and **20** show a small improvement in cellular permeability (without category change) in comparison with compound **1b** in our PAMPA model. We assessed rates of transport across MDCK-MDR1 (models of blood-brain barriers) monolayers in both directions (apical to basolateral (A-B) and baso-lateral to apical (B-A)) across the cell monolayer which enables us to determine the efflux ratio and shows if the compound undergoes active efflux. Studied conjugates **15**–**22** reported a low possibility to be absorbed to cross MDCK-MDR1 monolayers and were actively exported from the cells as indicated by efflux ratios >2.

2.2.3. Cell death evaluation based on Annexin V/PI double labeling

To study the cell death mode of selected highly cytotoxic compounds in more detail, we used Annexin V/PI labeling, allowing distinguishing cells in early or late phases of apoptosis and also necrotic cell death. We treated CCRF-CEM cells by **1b**, **8**, **21**, **22**, **23**, and **24** at $1 \times$ IC$_{50}$ or $5 \times$ IC$_{50}$ concentrations for 24 h followed by Annexin V/PI staining. Regarding evaluation, apoptotic cells were considered to be those stained with Annexin V alone (early apoptotic) or double stained with Annexin V and PI (late apoptotic; Fig. 3). Necrotic cells were positive only for PI staining. Among compounds tested, **21** proved strongest apoptotic activity, even at $1 \times$ IC$_{50}$ concentration, leading to more than 20-fold increase of apoptotic cells population compared to the untreated control. This result indicates very good anticancer activity of **21** through apoptosis induction. We further found massive apoptotic induction following treatment with **8** and **22** at $5 \times$ IC$_{50}$ concentration. The effect of other compounds was no or only marginal.

2.2.4. Effect of 1b, 8, 21, 22, 23, and 24 on the expression of apoptosis- and cell cycle-related proteins

To elucidate the mechanism by which the studied compounds induce apoptosis, the immunodetection of several proteins belonging to programmed cell death pathways was performed (Fig. 4). Accumulation of

Table 3
Pharmacological parameters of compounds **1b**, **1c**, **2b**, **2c**, and **8**.

Compound	Chemical stability				Plasma stability				
	% Compound remaining				% Compound remaining				
	15 min	30	60	120	15 min	30	60	120	
1b	101.41	97.01	89.57	91.10	101.67	99.64	105.90	91.61	
1c	85.92	87.29	75.32	81.37	97.30	100.06	95.03	88.92	
2b	100.77	101.96	93.63	98.45	103.64	102.86	100.28	87.28	
2c	92.56	92.48	90.66	97.62	98.29	95.06	87.33	88.07	
8	98.04	95.48	93.01	93.45	99.9	99.0	93.1	86.32	

	Microsomal stability				Microsomal stability				
	% Compound remaining				Category of Intrinsic clearence[a]				
Compound	15 min	30	60						
1b	96.87	83.28	43.27		Medium				
1c	98.80	101.89	92.28		Low				
2b	102.08	88.24	79.48		Low				
2c	90.25	71.93	52.64		Medium				
8	98.32	92.37	77.27		Medium				

Compound	Plasma protein binding	PAMPA		MDCK-MDR1 Permeability Assay				
	% Fraction bound	log Pe	Category[b]	Papp (x10e-6)	Category	Efflux ratio	active efflux	% recovery
1b	98.8	−7.64	Low	0.33	negative	1.73	No	99.63
1c	90.0	−7.44	Low	0.21	negative	0.6	No	103.79
2b	89.2	−7.04	Low	0.30	negative	0.96	No	46.46
2c	90.0	−7.78	Low	0.29	negative	0.34	No	49.52
8	99.69	−6.07	Low	1.54	negative	0.94	No	105.6

[a],[b] References [28,29], error deviations are ranges of values lower than 10% (all experiments were done in triplicates except cell-based permeability assay were done in duplicates).

Table 4
Pharmacological parameters of compounds 15–22.

Compound	Chemical stability				Plasma stability					
	% Compound remaining				% Compound remaining					
	15 min	30	60	120	15 min	30	60	120		
15	98.54	92.67	82.35	77.88	94.26	92.19	87.79	83.37		
16	92.04	84.77	82.55	82.34	99.56	99.27	97.76	96.09		
17	97.06	92.49	89.21	83.77	93.87	88.70	86.95	82.3		
18	98.39	93.00	93.23	85.98	99.02	96.13	88.71	86.31		
19	98.91	99.54	92.14	92.9	98.72	91.16	88.03	87.06		
20	91.19	89.20	87.13	86.84	98.62	94.8	93.5	87.37		
21	99.93	91.12	87.81	85.16	103.99	97.20	88.74	88.52		
22	94.63	93.41	91.67	90.67	97.09	97.77	91.80	90.03		

Compound	Microsomal stability				Microsomal stability					
	% Compound remaining				Category of Intrinsic clearence[a]					
	15 min	30	60							
15	99.03	98.82	96.97		Low					
16	67.23	59.39	42.28		Medium					
17	95.56	82.70	66.63		Medium					
18	89.94	83.67	81.83		Low					
19	99.28	98.30	97.85		Low					
20	95.62	83.65	77.80		Low					
21	96.77	95.71	58.86		Medium					
22	96.02	91.47	73.34		Medium					

Compound	Plasma protein binding	PAMPA		MDCK-MDR1 Permeability Assay				
	% Fraction bound	log Pe	Category[b]	Papp (x10e-6)	Category	Efflux ratio	active efflux	% recovery
15	99.56	−7.44	Low	0.28	negative	5.61	Yes	77.00
16	98.68	−7.30	Low	0.16	negative	4.30	Yes	98.18
17	99.85	−7.58	Low	0.32	negative	3.77	Yes	103.04
18	99.76	−7.26	Low	0.17	negative	8.88	Yes	105.48
19	89.25	−6.96	Low	1.67	negative	7.10	Yes	87.72
20	99.73	−6.98	Low	0.12	negative	3.7	Yes	82.19
21	99.83	−7.82	Low	0.12	negative	4.49	Yes	77.62
22	99.29	−5.57	Medium	1.05	negative	9.60	Yes	99.15

[a,b] Reference [28,29], error deviations are ranges of values lower than 10% (all experiments were done in triplicates except cell-based permeability assays were done in duplicates).

Bax and Bid, key components for cellular apoptosis induced through mitochondrial stress, was found out after 24 h treatment with studied triterpene derivatives. Upon apoptotic stimulation, Bax forms oligomers or interacts with Bid and translocates from the cytosol to the mitochondrial outer membrane [30]. Through interactions with pore proteins on the mitochondrial membrane, Bax and Bax/Bid complexes increase the membrane permeability, which ultimately leads to the release of cytochrome *c* from mitochondria and subsequent apoptosome complex formation with Apaf-1 and pro-caspase-9 and resulting in caspase-9 activation [31]. Immunodetection of Bax revealed a presence of its cleavage products which more potently induces apoptosis as indicated by higher cytochrome *c* release, caspase-3/7 activation, and DNA fragmentation, potentially due to their increased homo-oligomerization in mitochondrial membranes [32]. Thus, Bax and Bid pro-apoptotic proteins relay an apoptotic signal from the cell surface to the mitochondria triggering caspase activation [33]. Thus, we further concentrated on critical executioners of apoptosis including caspase-3 and caspase-7, as they are either partially or totally responsible for the proteolytic cleavage of many key proteins, such as the nuclear enzyme poly (ADP-ribose) polymerase (PARP). PARP, a 116 kDa nuclear poly (ADP-ribose) polymerase, appears to be involved in DNA repair in response to environmental stress [34]. This protein can be cleaved by many ICE-like caspases *in vitro* [35] and is one of the main cleavage targets of caspase-3 *in vivo* [36]. In human PARP, the cleavage occurs between Asp214 and Gly215, which separates the PARP amino-terminal DNA binding domain (24 kDa) from the carboxy-terminal catalytic domain (89 kDa) [36]. PARP helps cells to maintain their viability; cleavage of PARP facilitates cellular disassembly and serves as a marker of cells undergoing apoptosis. The obvious cleavage of PARP was detected in CCRF-CEM cells treated with compounds at these

concentrations: $1 \times IC_{50}$ and $5 \times IC_{50}$ **8**, $1 \times IC_{50}$ and $5 \times IC_{50}$ **21**, $1 \times IC_{50}$ and $5 \times IC_{50}$ **22**, $5 \times IC_{50}$ **24**, $5 \times IC_{50}$ **23**. Furthermore, we focused on the levels of proteins belonging to the "BH3-only" family. Members of the "BH3-only" family (e.g. Noxa, Bad, Bim, Puma, Bid, Bik, and Hrk) are highly regulated proteins that induce apoptosis through BH3-dependent interaction with anti-apoptotic Bcl-2 family proteins [37]. First of all, we chose Noxa, a small protein that plays a key role in mediating apoptotic signaling. It contains a single Bcl-2 homology (BH3) domain [38] and localizes to mitochondria where it binds the anti-apoptotic proteins Mcl-1 and A1/Bfl-1 [39]. It also competes with Mcl-1 for binding to mitochondrial Bak protein. The increased expression of Noxa nicely correlates with cleaved PARP and indicates ongoing apoptosis as a result of triterpene's effect on CCRF CEM cells. Further, we concentrated on Bim which similarly to Noxa contains a BH3 domain and induces apoptosis by binding to and antagonizing anti-apoptotic members of the Bcl-2 family, namely Bcl-2, Bcl-xL, Mcl-1, Bcl-w, Bfl-1, and BHRF-1 [40]. Finally, c-Myc, a marker of increased cellular proliferation which is frequently induced in many cancer types was immunodetected [41]. Its expression was markedly decreased as a response to treatments with triterpene derivatives: $1 \times IC_{50}$ and $5 \times IC_{50}$ **8**, $1 \times IC_{50}$ and $5 \times IC_{50}$ **21**, $5 \times IC_{50}$ **22**, $5 \times IC_{50}$ **23**. This finding goes hand in hand with data from cell cycle analysis where an accumulation of cells in sub-G_1 and G_0/G_1 phases were detected at the expense of S, G_2, and M phases.

2.2.5. The cells' treatment by compounds 1b and 8 results in the fast damage of mitochondria

As our data indicated that the mitochondrial stress could play important role in the toxicity of the tested compounds, we treated CCRF-CEM and HeLa cells with 10 μM compound **1b** or **8** for 4 h. Mitochondria
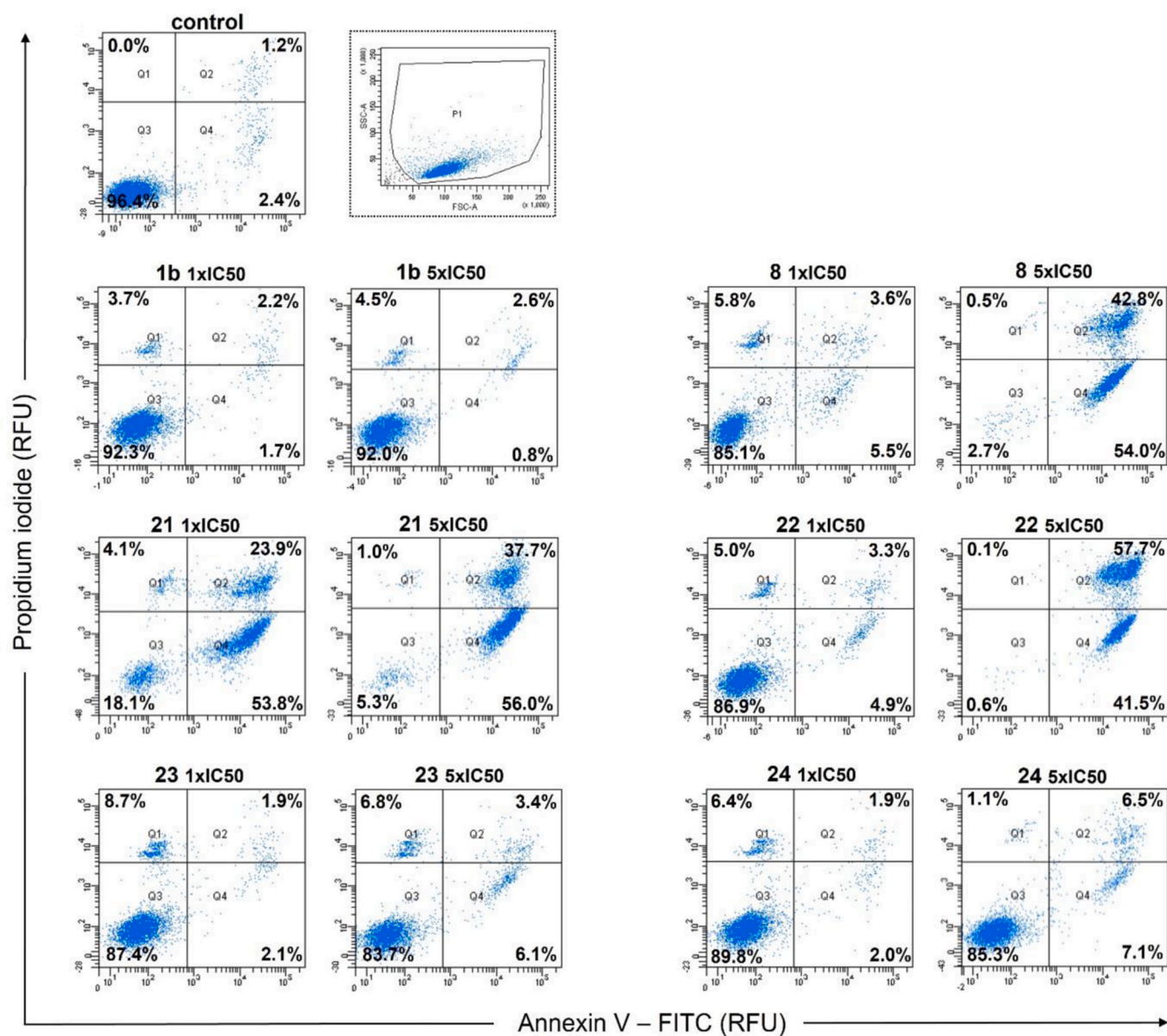
Fig. 3. Representative dot plot diagrams of dual Annexin V/Propidium iodide staining of CCRF-CEM cells treated with **1b**, **8**, **21**, **22**, **23**, and **24** at $1 \times IC_{50}$ and $5 \times IC_{50}$ concentrations for 24 h. Prior to analysis, dead cells and debris were gated out by forward scatter versus side scatter gating (upper picture marked with dotted line). Then, cells from P1 gate were projected to red/green channels dot-plot diagram. The fluorescence signal was measured at green (FITC Annexin V) and red (PI) channels using FACSAria II flow cytometer. At least 10 000 cells were acquired in each sample and analysis of individual quadrants was performed. The percentage calculation of viable (Q3 area), early apoptotic (Q4), late apoptotic (Q2) and necrotic (Q1) cells has been evaluated based on appropriate coordinates setting.

were visualized in the formaldehyde-fixed cells using antibody recognizing MT-CO2 [42], a cytochrome *c* oxidase subunit 2 [43].

We included HeLa cells in this part of the study as mitochondria of HeLa cells are organized into well-discerned chains (Fig. 5, upper panel). The sensitivity of HeLa cells to both compounds is relatively low as IC50 for the compound **1b** and **8** was 11.9 and 5.63 μM, respectively. In this respect, we firstly tested impact of various concentrations of both compounds on the mitochondria of HeLa cells. In the case of the compound **1b**, 1, 5, 10, 20, or 50 μM concentration was analyzed, in the case of more toxic compound **8**, 0.5, 2.5, 5, 10 or 20 μM concentration was tested. As HeLa cells are adherent, they can be cultivated on glass coverslips. Therefore, the eventual impact of the tested compounds on mitochondria can be easily identified by the fluorescence microscopy. CCRF-CEM cells grow in suspension, and their processing requires the cytocentrifugation steps. In addition, mitochondria of rounded CCRF-CEM cells occupy relatively small area at high mitochondria density

(Fig. 5, lower panel) further complicating their analysis.

Clear differences between mitochondria's organization were observed in HeLa cells (Fig. 5, upper panel) if 10 μM or higher concentrations of both compounds were used. On the other hand, no such effect was observed in the case of CCRF-CEM cells (Fig. 5, lower panel) although we used relatively high concentration of both compounds (~more than $10 \times$ of the IC_{50} concentration).

To distinguish whether the difference between HeLa and CCRF-CEM cells can be attributed to the distinct effect of the tested compounds on various cell types, or it is a result of insufficient resolution of mitochondria in CCRF-CEM cells, we further performed electron microscopy (EM) analysis of the CCRF-CEM cells treated or non-treated with 10 μM compound **1b** (Fig. 6). It is obvious from the Fig. 6 that the treatment of cells with the compound **1b** resulted into profound changes of mitochondria organization as mitochondrial cristae were dramatically changed (Fig. 6).
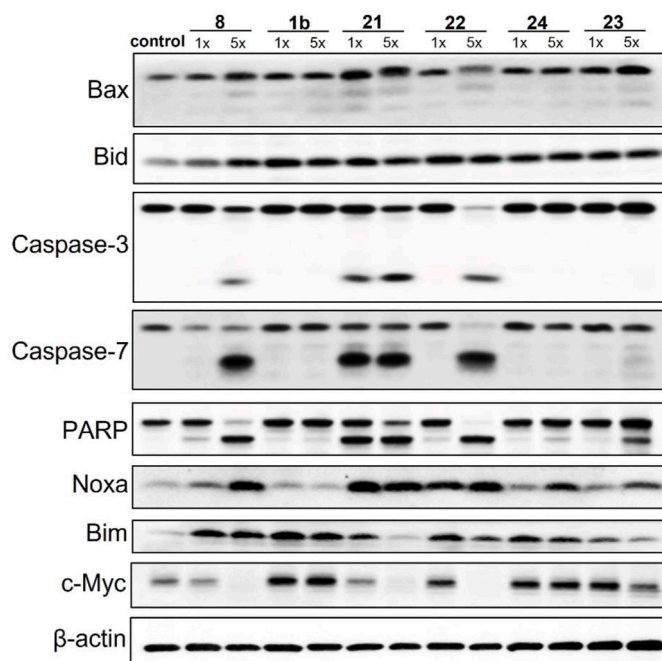
Fig. 4. Western blot analysis of CCRF-CEM cells treated by **8**, **1b**, **21**, **22**, **24**, and **23** at $1 \times IC_{50}$ and $5 \times IC_{50}$ concentrations for 24 h. For the caspases-3/7 detection, antibodies specifically recognizing both, precursor and active form were used. Using *anti*-PARP antibody, full-length protein, as well as fragment produced by caspase cleavage, was detected. To check equal amount of proteins loaded per well, anti β-actin antibody was used. The untreated cells were taken as a control. Relative concentration of each pyridine/pyrazine in CCRF-CEM and CEM-DNR cells.

For the direct visualization of the sites in the cell that contain compound **1b** or **8**, we used their propargylic esters **13** and **14** that are ready for the click reaction with azides. In these experiments, cells were incubated with 10 μM compounds **13** or **14** (propargylic derivatives of the compounds **1b** and **8,** respectively) for 4 h, fixed and the tested compounds were visualized by click reaction catalyzed by the monovalent copper ions. Simultaneously, MT-CO2 was visualized by antibody detection. We observed significant overlap of MT-CO2 marker and compound **14** signal in the case of HeLa cells (Fig. 7). If compound **13** was used, no signal was observed after click reaction. In this case, we also did not observe damaged mitochondria as in the case of **1b** compound. It indicates that the replacement of COOH group by the propargyl group could inactivate the compound **13** or could prohibit the transport of the compound **13** into cells. It was in agreement with our results obtained with CCRF-CEM cells. In this case, we also did not observe any signal after click reaction with compound **13**. When compound **14** was analyzed, we observed partial co-localization of compound **14** signal and MT-CO2 signal. However, contrary to HeLa cells, it was not so clearly visible due to the organization of mitochondria in CCRF-CEM cells.

In summary, all these data indicate that mitochondria are an important target of the compounds **1b** and **8** action.

2.2.6. Effect of selected compounds in spheroid cultures

The effects of compounds **1b**, **8**, **17**, and **21** were next tested in spheroid cultures of HCT116 and HeLa cells to determine their activity in pathophysiologically relevant *in vitro* tumor models [44]. All derivatives significantly inhibited growth and resulted in the complete disintegration of spheroids of both cell types at the highest tested 10 μM concentration (Fig. 8 A). Both **1b** and **21** resulted in dose-dependent growth inhibition and a partial opening of spheroids at 1 μM in HeLa cell spheroids (Fig. 8 B). Although we did not examine the mechanisms

of drug effect in spheroids, triterpenes are known to target HIF-1α, effectively reproduced in spheroids, and EGFR, which stimulates spheroid formation [45–47]. The ability of **1b** and **21** to cause the opening of spheroids can potentially help the penetration of other less-penetrating cytotoxic drugs in tumors during combination therapy.

3. Conclusions

In this work, we investigated a set of triterpenic pyridines and pyrazines **1b**–**8** with cytotoxic activity. Among them, compounds **1b**, **1c**, **2b**, **2c**, and **8** had the IC_{50} in high nanomolar or low micromolar range of concentration and were further developed. The contribution of the parent triterpene and pyrazine or pyridine part to the cytotoxicity of resulting heterocyclic terpenes seems to be synergic. The derivatives of lupane and taraxastane prepared in this work are selectively cytotoxic, while derivatives of 18α-oleanane are inactive which is in agreement with our earlier work [8,11]. Derivatives of ursane and oleanane were moderately active, so it is difficult to make any strong conclusion about the SAR among them. Terpenic pyrazines are not truly bioisosteric with pyridines because most active compounds have activity in different cancer cell lines, pyrazines **1b**, **2b**, and **6b** are cytotoxic on CCRF-CEM cell line while pyridines **1c**, **2c**, and **6c** are cytotoxic on daunorubicin resistant CEM-DNR and taxol resistant K562-TAX line.

After the initial screening, pharmacological parameters of the most active compounds were measured. Molecules **1b**, **1c**, **2b**, **2c**, and **8** had excellent chemical, plasma, and microsomal stability; however, it was necessary to consider which kind of modification could achieve better cell permeability and/or selectivity in case of compound **8**. Compounds **1b** and **8** were selected as model examples for conjugation with glucose analogs in order to increase the polarity and thus, to optimize their bioavailability. The resulting conjugates **15**–**21** had similar ADME properties to the parent compounds, only compound **22** had better permeability in PAMPA model. 30-Oxoderivatives **12**, **17**, and **21** (prepared from **8**) were found to be active (IC_{50} in all cancer cell lines 0.60–2.7 μM) but they remained unselective (TI 2.8–5.0). In contrast, 30-oxoderivatives **14**, **18**, and **22** remained active in CCRF-CEM cell line (IC_{50} 0.43–4.6 μM) and gained selectivity, since they are less active in both fibroblast lines but also in several cancer cell lines (TI > 10). Conjugates **15**, **16**, **19**, **20** lost the activity.

Second, a set of medoxomil prodrugs **23**–**28** was synthesized to improve the bioavailability of the parent compounds. Medoxomil prodrug was described to be metabolized *in vivo* to obtain an active parent acid [22]. Conjugates **23**–**28** were prepared from the starting acids **1a** and **9** and from the most interesting compounds **1b**, **1c**, **2b**, **2c**. It was found that resulting compounds **23**, **24**, and **25** are active in CCRF-CEM cell line with sufficient selectivity. In addition, compounds**24**, and **26**–**28** are significantly active against the myelognous leukemia cell line K562 with IC_{50} between 0.037 and 0.87 μM and their selectivity is very high. Concerning cytotoxicity across the entire panel of cancer cell lines used and compounds tested, compounds **26**–**28** are to date the most active triterpenes prepared in our lab.

Third, the mechanism of action of selected compounds was tested. Annexin V/propidium iodide staining experiment revealed, that compounds **1b**, **8**, **21**, **22**, **23**, and **24** cause selective apoptosis in CCRF-CEM cells with the most significant effect in compounds **8**, **21**, and **22**. It is well documented, that mitochondria represent the main cellular target for triterpenes. Therefore, detailed analysis of the Bcl-2 family members, representing key regulators of mitochondrial pathway of apoptosis, has been performed. First, we concentrated on multidomain pro-apoptotic proteins Bax and Bid, influencing mitochondrial membrane permeability. All the compounds caused significant up-regulation of Bax as well as Bid proteins. Further, we studied effect of compounds on expression of selected proteins belonging to "BH3-only" subgroup with antagonizing function to anti-apoptotic proteins from Bcl-2 family. We found, that **8**, **21** and **22** dramatically increase expression of Noxa protein and moreover, all compounds significantly increased Bim
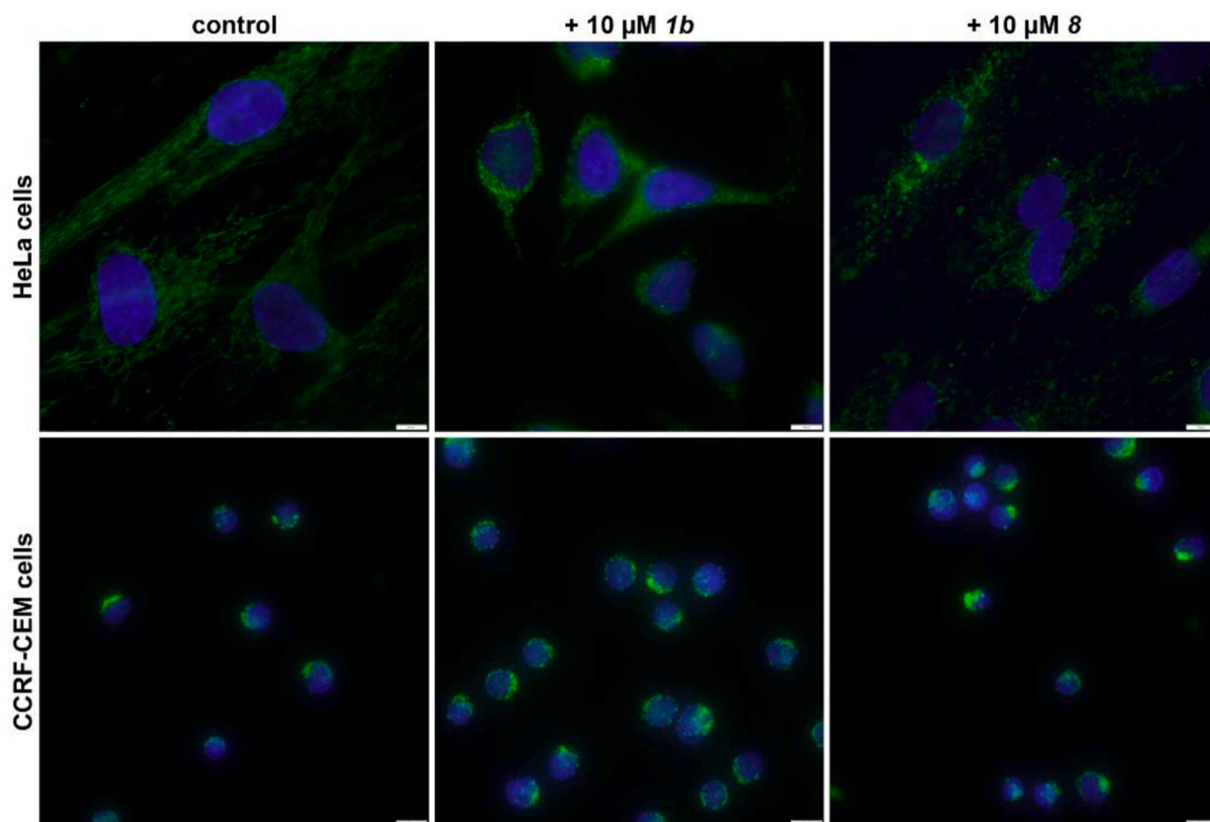
Fig. 5. Light microscopy (LM) analysis of the impact of compounds **1b** and **8** on mitochondria in HeLa cells (upper panel) and CCRF-CEM cells (lower panel). Cells were incubated without (control) or with 10 μM compound **1b** or **8** and processed for fluorescence microscopy. Mitochondria were stained by MT-CO2 marker (green), cell nuclei by DAPI (blue). Scale bar = 10 μm.
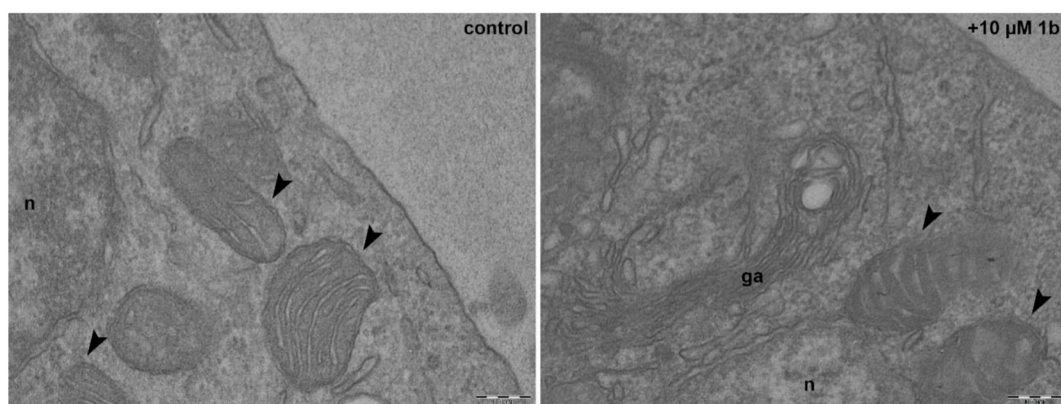

Fig. 6. EM analysis of the impact of compound **1b** on mitochondria in CCRF-CEM cells. CCRF-CEM cells were incubated without (left panel) or with (right panel) 10 μM compound **1b** and processed for electron microscopy. 70-nm sections were cut from the epon-embedded samples and post-contrasted by 3% uranyl acetate. **n** = nucleus; **ga** = Golgi apparatus; **arrowheads** indicated mitochondria. Scale bar = 0.2 μm.

expression. Finally, we explored effect of compounds on the main execution caspases-3/7 and PARP, as a representative of their downstream substrates. We found obvious caspase-3/7 activation induced by **8**, **21** and **22**, as documented by reduced level of precursor forms and presence of their active forms and well corresponding PARP cleavage. All these results nicely correlate with Annexin V measurement.

In order to obtain further insight into the interaction of our compounds with mitochondria, structures **1b** and **8** were treated to CCRF-CEM and HeLa cells to visualize their effects within the living cell using light fluorescent microscopy. Both compounds were found to interfere with the mitochondria of HeLa cells with stronger effect in compound **8**. Since this effect was not possible to be observed in CCRF-

CEM cells using the light fluorescent microscopy due to their tight clusters, an additional experiment was performed using the electron microscopy. These experiments confirmed, that compound **1b** causes changes in mitochondria organization in CCRF-CEM cells as well. Propargyl esters **13** and **14** were prepared from compounds **1b** and **8** and used for the direct visualization of the cellular targets of both compounds. Clear co-localization of compound **14** with mitochondria marker MT-CO2 in both CCRF-CEM and HeLa cells was observed. On the other hand, no signal was observed with compound **13**. This may be explained by the fact that free 28-COOH group of triterpenic acids is usually important for their activity and since here it was used for the introduction of the propargyl group, it diminished the activity/cell
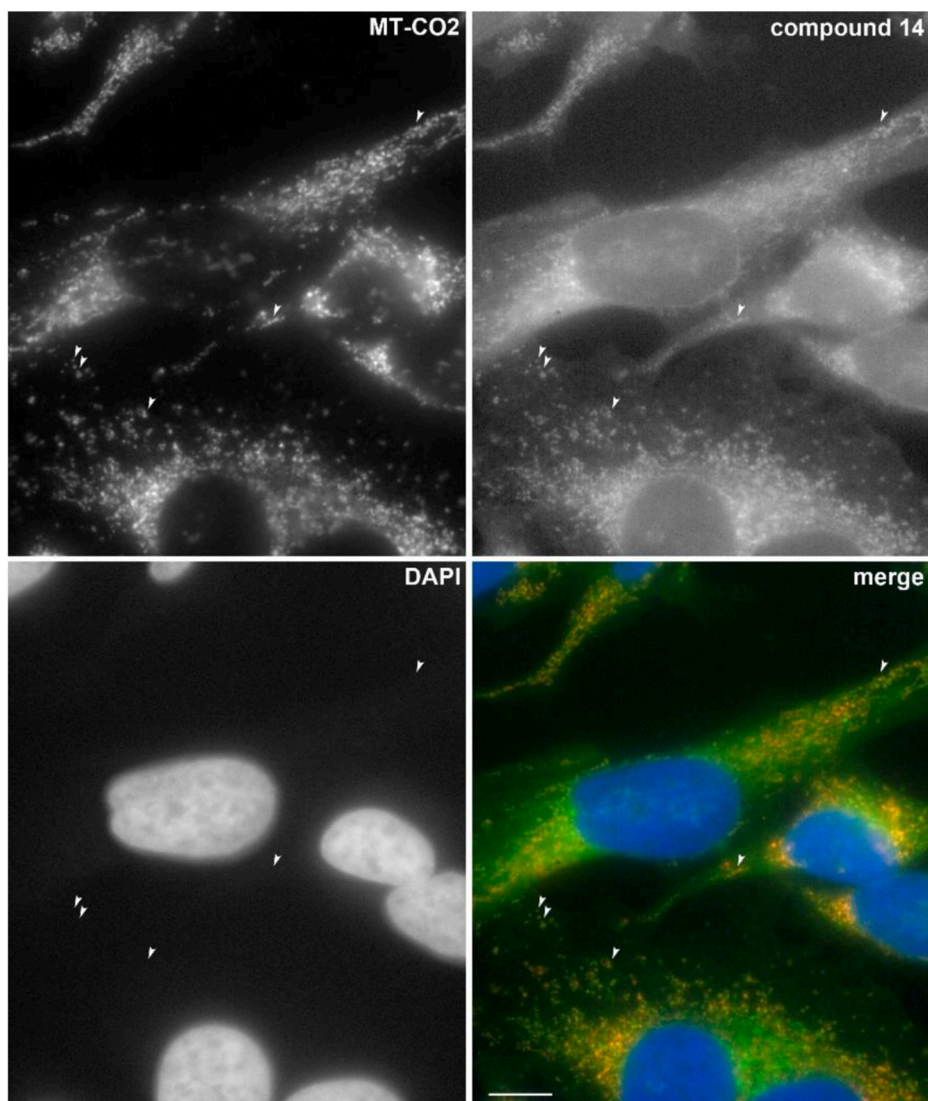
Fig. 7. Detection of compound **14** by click reaction. HeLa cells were incubated with 10 μM compound **14** for 4 h. Compound **14** was detected by copper-catalyzed click reaction with 5-FAM azide (green in merged figure). Simultaneously, mitochondrial marker MT-CO2 (red in merged figure) and nuclear DNA (blue in merged figure) were visualized. Scale bar = 10 μm.

permeability for the compound **13** while some activity remained in the more cytotoxic analogous derivative **14**.

As a further step towards anticancer drug development, the effects of compounds **1b**, **8**, **17**, and **21** in spheroid cultures of HCT116 and HeLa cells were tested to determine their activity in pathophysiologically relevant *in vitro* tumor models. All derivates significantly inhibited growth and resulted in the complete disintegration of spheroids of both cell types at the highest tested 10 μM concentration. Compounds **1b** and **21** resulted in dose-dependent growth inhibition and a partial opening of spheroids at 1 μM in HeLa cell spheroids which can potentially help the penetration of other less-penetrating cytotoxic drugs in tumors during combination therapy.

To sum up, a small library of triterpenoid pyridines and pyrazines was prepared and based on their ADME parameters, more derivatives were obtained to improve their cell permeability and selectivity. Among all synthesized compounds, the medoxomil prodrugs **23**–**28** had activity in low nanomolar concentration range and these compounds will be included in the future *in vivo* tests to determine their behavior in living organisms and to show if it is worth to use this prodrug moiety. Compounds **1c**, **2b**, and **2c** are significantly more active in daunorubicin resistant CEM-DNR cells and in taxol resistant K562-Tax cells which

deserves thorough studies in the future. All studies of the mechanism of action show that the active compounds cause selective apoptosis *via* intrinsic pathway.

Future directions. Compounds **1b**, **1c**, **2b**, **2c**, **24**, and **26**–**28** were selected as the most promising structures for further drug development because of their low IC$_{50}$ and high selectivity. Especially the medoxomil prodrugs **24**–**28** will require *in vivo* tests to prove their usefulness. Compounds **1c**, **2b**, and **2c** will be studied because of their selectivity against resistant cancer cell lines.

4. Experimental procedures

4.1. Chemistry

Melting points were determined using either the Büchi B-545 apparatus or the STUART SMP30 apparatus and are uncorrected. Optical rotations were measured on an Autopol III (Rudolph Research, Flanders, USA) polarimeter in MeOH at 25 °C and are in [10^{-1} deg cm^2 g^{-1}]. Infrared spectra were recorded on a Nicolet Avatar 370 FTIR and processed in the OMNIC 9.8.372. DRIFT stands for Diffuse Reflectance Infrared Fourier Transform. ^{1}H and ^{13}C experiments were performed on
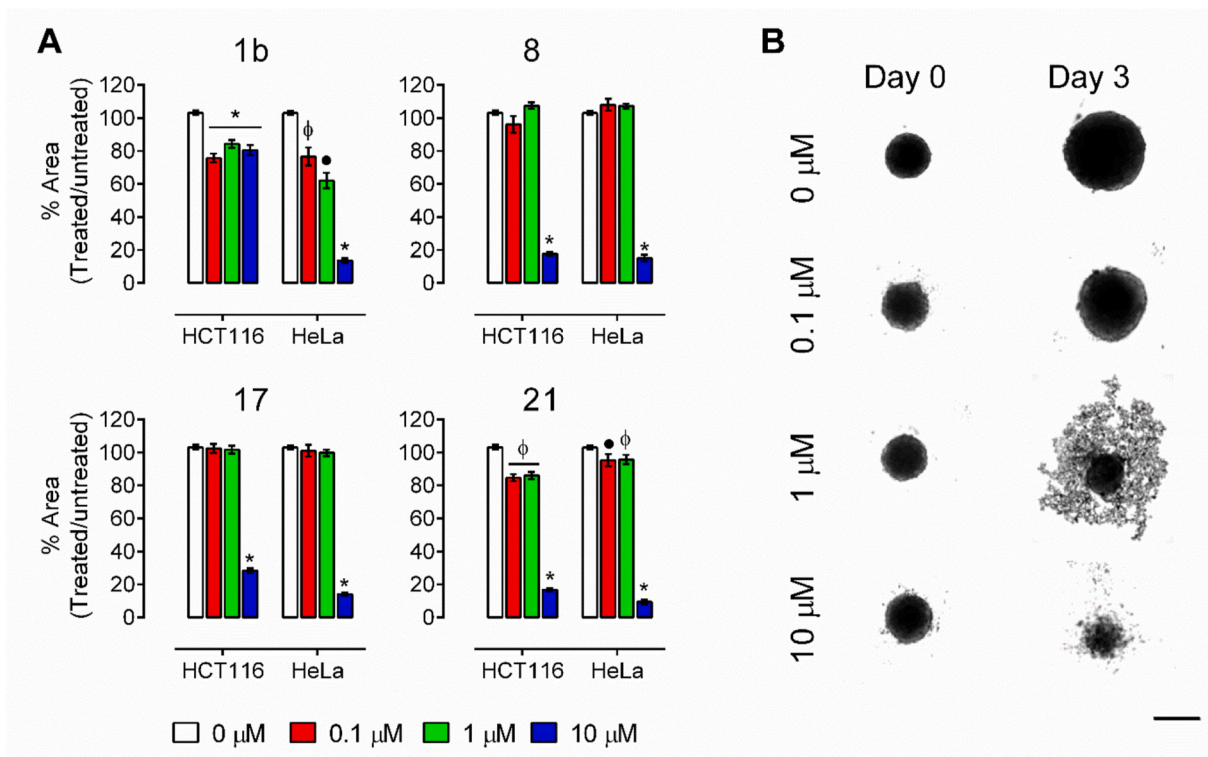
Fig. 8. Derivative effect in 3D spheroid cultures. (A) Graphs showing the change in the size (area) of spheroids of HCT116 and HeLa cells following treatment with the **1b**, **8**, **17** and **21** at indicated concentrations. n = 3 independent experiments, *p < 0.001, ● p < 0.01, φ p < 0.05 *vs* 0 μM (Control), one-way ANOVA, Sidak's multiple comparisons test. (B) Representative images showing HeLa spheroids before the start of drug treatment (Day 0) and 3 days after treatment with **21**. Note the opening of spheroids at 1 μM and complete disintegration of spheroids at 10 μM. Scale bar: 100 μm, n = 3 independent experiments.

Jeol ECX-500SS (500 MHz for ^{1}H), and Varian^{UNITY} Inova 400 (400 MHz for ^{1}H) instruments, using CDCl$_3$, DMSO-d_6, CD$_3$OD or THF-d_8 as solvents (25 °C). Chemical shifts (δ) were referenced to the residual signal of the solvent (CDCl$_3$, DMSO-d_6, CD$_3$OD or THF-d_8) and are reported in parts per million (ppm). Coupling constants (J) are reported in Hertz (Hz). NMR spectra were processed in the ACD/NMR Processor Academic Edition 12.01, MestReNova 6.0.2–5475 or JEOL Delta v5.0.5.1. EI-MS spectra were recorded on an INCOS 50 (Finnigan MAT) spectrometer at 70 eV and an ion source temperature of 150 °C. The samples were introduced from a direct exposure probe at a heating rate of 10 mA/s. Relative abundances stated are related to the most abundant ion in the region of $m/z > 180$. HRMS analysis was performed using an LC-MS Orbitrap Elite high-resolution mass spectrometer with electrospray ionization (Dionex Ultimate 3000, Thermo Exactive plus, MA, USA). Spectra were taken at the positive and negative mode in the range of 400–700 m/z. The samples were dissolved in MeOH and injected to the mass spectrometer over autosampler after HPLC separation: precolumn Phenomenex Gemini (C18, 50 × 2 mm, 2.6 μm), mobile phase isocratic MeOH/water/HCOOH 95:5:0.1. The course of the reactions was monitored by TLC on Kieselgel 60 F$_{254}$ plates (Merck) detected first by UV light (254 nm) and then by spraying with 10% aqueous H$_2$SO$_4$ and heating to 150 °C-200 °C. Purification was performed using column chromatography on Silica gel 60 (Merck 7734).

Betulonic acid (**1a**), dihydrobetulonic acid (**2a**), oleanonic acid (**3a**), moronic acid (**4a**), ursonic acid (**5a**), heterobetulonic acid (**6a**), and allobetulon (**7a**) were purchased from company Betulinines (www.betulinines.com), which manufactures them from betulin, betulinic acid and oleanolic acid in bulk scale. All other chemicals and solvents were obtained from Sigma-Aldrich, Lachner or Across Chemicals.

4.2. General procedure for preparing pyridines (procedure A)

The procedure was adopted from the lit [9,13]. and slightly modified. To a stirred solution of 3-oxotriterpenes **1a–7a** in dry EtOH was added propargylamine (5 equiv.), CuCl (0.6 equiv.) and activated molecular sieves (3 Å). Reaction mixture was stirred in reaction vial for 48–120 h at 80 °C and monitored by TLC (toluene/diethyl ether 5 : 1, UV detection). Then the reaction mixture was filtered, the solvent was evaporated and the crude brown product was purified by column chromatography (toluene/diethyl ether 10 : 1). The final products **1c–7c** were obtained as white solid.

4.2.1. Lup-2-eno [2,3-b]pyridine-28-oic acid 2c

Compound 2c was prepared according to the general procedure **A**, the reaction time was 120 h and the product was crystallized from CHCl$_3$/MeOH to give 188 mg (35%) of pyridine **2c**: m. p. 142–143 °C; ^{1}H NMR (500 MHz, CDCl$_3$) δ: 0.75–0.81 (m, 6H), 0.88 (d, 3H, $J = 6.8$ Hz), 1.00 (d, 6H, $J = 6.4$ Hz), 1.28 (s, 3H), 1.32 (s, 3H, 7 × CH$_3$), 1.83 (td, 1H, $J_1 = 6.8$ Hz, $J_2 = 2.5$ Hz), 1.93 (dd, 1H, $J_1 = 12.2$ Hz, $J_2 = 7.5$ Hz), 2.31–2.34 (m, 1H, H-1a), 2.35–2.36 (m, 2H), 2.75 (d, 1H, $J = 15.8$ Hz, H-1b), 7.03 (dd, 1H, $J_1 = 7.6$, $J_2 = 4.8$ Hz), 7.27–7.30 (m, 1H), 8.47 (dd, 1H, $J_1 = 4.7$ Hz, $J_2 = 1.2$ Hz, 3 × H–pyridine); ^{13}C NMR (126 MHz, CDCl$_3$) δ: 14.70, 14.87, 15.85, 16.01, 20.39, 21.70, 22.98, 23.18, 27.15, 29.97, 31.51, 31.73, 32.36, 33.74, 36.32, 37.56, 38.41, 39.54, 40.75, 42.77, 44.31, 45.98, 48.71, 48.95, 53.70, 56.97, 120.05, 121.16, 130.25, 138.46, 146.77, 163.52, 180.64; IR (DRIFT) ν_{max}: 3530, 2866, 1693 cm^{-1}; HRMS (ESI$^+$) m/z calcd for C$_{33}$H$_{50}$NO$_2$ [M+H]$^+$ 492.3836, found 492.3835.

4.2.2. Oleana-2,12-dieno [2,3-b]pyridine-28-oic acid 3c

Compound 3c was prepared according to the general procedure **A**, the reaction time was 48 h and the product was crystallized from CHCl$_3$/MeOH to give 148 mg (27%) of pyridine **3c**: m. p. 168–169 °C; ^{1}H NMR (500 MHz, CDCl$_3$) δ 0.85 (s, 6H), 0.91 (s, 3H), 0.95 (s, 3H), 1.18 (s, 3H), 1.27 (s, 3H), 1.32 (s, 3H, 7 × CH$_3$), 1.79 (dd, 1H, $J_1 = 13.6$ Hz, $J_2 = 4.1$ Hz), 1.94–1.99 (m, 1H, H-11a), 1.99–2.07 (m, 2H), 2.39 (d, 1H, $J = 15.7$

Hz, H-1a), 2.67 (d, 1H, *J* = 15.8 Hz, H-1b), 2.90 (dd, 1H, *J₁* = 13.8 Hz, *J₂* = 4.1 Hz, H-11b), 5.35 (t, 1H, *J* = 3.4 Hz, H-12), 7.01 (dd, 1H, *J₁* = 7.6 Hz, *J₂* = 4.8 Hz), 7.26–7.29 (m, 1H), 8.47 (dd, 1H, *J₁* = 4.6 Hz, *J₂* = 1.1 Hz, 3 × H–pyridine); ^{13}C NMR (126 MHz, CDCl₃) δ: 14.10, 15.03, 16.93, 20.25, 22.63, 23.09, 23.41, 24.20, 25.70, 27.75, 30.71, 31.57, 32.23, 32.50, 33.11, 33.94, 36.02, 39.19, 41.25, 41.92, 45.45, 45.77, 45.96, 46.58, 53.53, 120.85, 122.30, 126.75, 137.86, 143.84, 146.90, 163.51, 182.60; IR (DRIFT) *ν*max: 3502, 1694 cm⁻¹; HRMS (ESI⁺) *m/z* calcd for C₃₃H₄₈NO₂ [M+H]⁺ 490.3680, found 490.3680.

4.2.3. Oleana-2,18(19)-dieno [2,3-b]pyridine-28-oic acid 4c

The general procedure **A** only yielded 5% of the product, therefore, a modification using different catalyst and slightly different conditions was used. Propargylamine (57.5 μL, 0.88 mmol) and NaAuCl₄·2H₂O (5 mg, 0.012 mmol) were added to a stirred solution of moronic acid **4a** (100 mg, 0.22 mmol) in EtOH (5 mL). Reaction mixture was stirred in a reaction vial for 48 h at 90 °C and the conversion of the starting acid was monitored by TLC (toluene/diethyl ether 5 : 1). The reaction mixture was filtered, the solvent was evaporated and the crude brown product was purified by column chromatography (toluene/diethyl ether 10 : 1 to 5 : 1). The final product **4c** was obtained as white solid, 46 mg (41%): m. p. 232–234 °C; ^{1}H NMR (500 MHz, CDCl₃) δ: 0.82 (s, 6H), 0.99 (s, 3H), 1.02 (s, 3H), 1.06 (s, 3H), 1.29 (s, 3H), 1.35 (s, 3H, 7 × CH₃), 2.03 (dm, 1H, *J* = 13.7 Hz), 2.21 (dt, 1H, *J₁* = 13.0 Hz, *J₂* = 3.0 Hz), 2.32 (d, 1H, *J* = 11.7 Hz), 2.38 (d, 1H, *J* = 15.7 Hz), 2.82 (d, 1H, *J* = 15.8 Hz), 5.18 (s, 1H, H-19), 7.05 (dd, 1H, *J₁* = 7.0 Hz, *J₂* = 5.0 Hz), 7.33 (d, 1H, *J* = 7.2 Hz), 8.52 (d, 1H, *J* = 4.0 Hz, 3 × H–pyridine); ^{13}C NMR (126 MHz, CDCl₃) δ: 15.00, 15.99, 16.29, 20.21, 21.70, 24.02, 26.21, 29.26, 29.52, 30.56, 31.56, 32.22, 33.57, 33.67, 33.69, 33.84, 36.39, 39.56, 40.67, 41.59, 42.75, 46.21, 48.17, 49.56, 53.84, 121.13, 130.31, 133.15, 137.14, 138.65, 146.79, 163.58, 181.25; IR (DRIFT) *ν*max: 2340–3680, 2933, 2863, 1696, 1583, 1449 cm⁻¹; HRMS (APCI) *m/z* calcd for C₃₃H₄₈NO₂ [M+H]⁺ 490.3680, found 490.3680.

4.2.4. Ursa-2,12-dieno [2,3-b]pyridine-28-oic acid 5c

Compound **5c** was prepared according to the general procedure **A**, the reaction time was 96 h and the product was crystallized from CHCl₃/ MeOH to give 155 mg (28%) of pyridine **5c**: m. p. 185–187 °C; ^{1}H NMR (500 MHz, CDCl₃) δ: 0.86 (s, 3H), 0.87 (s, 3H), 0.89 (d, 3H, *J* = 6.5 Hz), 0.95 (d, 3H, *J* = 6.4 Hz), 1.13 (s, 3H), 1.27 (s, 3H), 1.31 (s, 3H, 7 × CH₃), 1.79 (dt, 1H, *J₁* = 12.9 Hz, *J₂* = 3.2 Hz), 1.92 (td, 1H, *J₁* = 13.6 Hz, *J₂* = 4.1 Hz), 2.05–2.08 (m, 1H, H-11a), 2.05 (m, 2H), 2.27 (d, 1H, *J* = 11.3 Hz, H-11b), 2.42 (d, 1H, *J* = 14.9 Hz, H-1a), 2.70 (d, 1H, *J* = 15.8 Hz, H-1b), 5.32 (t, 1H, *J* = 3.5 Hz, H-12), 7.00 (dd, 1H, *J₁* = 7.6 Hz, *J₂* = 4.7 Hz), 7.26 (dd, 1H, *J₁* = 7.8 Hz, *J₂* = 1.4 Hz), 8.47 (dd, 1H, *J₁* = 4.6 Hz, *J₂* = 1.3 Hz, 3 × H–pyridine); ^{13}C NMR (126 MHz, CDCl₃) δ: 14.25, 15.41, 17.16, 17.28, 20.37, 21.35, 22.79, 23.56, 24.41, 28.26, 30.92, 31.77, 31.83, 32.73, 36.11, 36.98, 39.00, 39.41, 39.56, 42.41, 45.78, 45.90, 48.19, 52.99, 53.73, 121.02, 125.70, 129.95, 137.97, 138.30, 147.06, 163.67, 182.61; IR (DRIFT) *ν*max: 3508, 1737, 1693 cm⁻¹; HRMS (ESI⁺) *m/z* calcd for C₃₃H₄₈NO₂ [M+H]⁺ 490.3680, found 490.3679.

4.2.5. Taraxasta-2,20(21)-dieno [2,3-b]pyridine-28-oic acid 6c

The general procedure **A** only yielded 5% of the product, therefore, a modification using slightly different conditions was used. Propargyl-amine (57.5 μL, 0.88 mmol), CuCl (5 mg, 0.05 mmol) and activated molecular sieve beads (0.5 g, 3 Å) were added to a stirred solution of heterobetulonic acid **6a** in EtOH (5 mL). The reaction mixture was stirred in a reaction vial for 48 h at 80 °C while the conversion of the starting material was monitored by TLC (tolu-ene/Et₂O 5 : 1, UV detection). Then the reaction mixture was filtered, the solvent was evaporated and the crude brown product was purified by column chromatography (toluene/Et₂O 10 : 1). The final product **6c** was obtained as white solid, 52 mg (48%): m. p. 121–123 °C; ^{1}H NMR (500 MHz, CDCl₃) δ: 0.79 (s, 3H), 0.99 (s, 3H), 1.01 (s, 3H), 1.02 (d, 3H, *J* = 6.6 Hz), 1.29 (s, 3H), 1.33 (s, 3H), 1.65 (s, 3H, 7 × CH₃), 1.81 (ddd, 2H,

J₁ = 15.0 Hz, *J₂* = 19.9 Hz, *J₃* = 2.3 Hz), 2.04 (dd, 1H, *J₁* = 10.1 Hz, *J₂* = 2.8 Hz), 2.15 (dd, 1H, *J₁* = 13.4 Hz, *J₂* = 6.7 Hz), 2.30 (dd, 1H, *J₁* = 15.5 Hz, *J₂* = 7.2 Hz), 2.38 (d, 1H, *J* = 15.7 Hz), 2.46 (td, 1H, *J₁* = 18.8 Hz, *J₂* = 3.2 Hz), 2.78 (d, 1H, *J* = 15.8 Hz), 5.30 (d, 1H, *J* = 7.0 Hz, H-21), 7.04 (dd, 1H, *J₁* = 7.6 Hz, *J₂* = 4.8 Hz), 7.31 (d, 1H, *J* = 7.4 Hz), 8.42–8.44 (m, 1H, 3 × H–pyridine); ^{13}C NMR (126 MHz, CDCl₃) δ: 14.93, 15.92, 16.02, 20.31, 21.91, 22.30, 23.56, 24.00, 27.51, 29.24, 31.50, 33.05, 33.53, 36.31, 37.44, 37.98, 39.27, 39.53, 40.86, 42.07, 46.07, 48.88, 49.05, 53.73, 117.02, 121.17, 130.33, 138.53, 143.37, 146.63, 163.50, 180.30; IR (DRIFT) *ν*max: 2450–3670, 2936, 2868, 1697, 1583, 1445 cm⁻¹; HRMS (APCI) *m/z* calcd for C₃₃H₄₈NO₂ [M+H]⁺ 490.3680, found 490.3680.

4.2.6. 19β,28-epoxy-18α-olean-2-eno [2,3-b]pyridine 7c

Compound **7c** was prepared according to the general procedure, the reaction time was 120 h and the product was crystallized from CHCl₃/ MeOH to give 122 mg (23%) of pyridine **7c**: m. p. 218–219 °C; ^{1}H NMR (500 MHz, CDCl₃) δ: 0.81 (s, 6H), 0.94 (s, 3H), 0.95 (s, 3H), 1.05 (s, 3H), 1.27 (s, 3H), 1.32 (s, 3H, 7 × CH₃), 2.37 (d, 1H, *J* = 15.8 Hz, H-1a), 2.77 (d, 1H, *J* = 15.6 Hz, H-1b), 3.46 (d, 1H, *J* = 7.8 Hz, H-28a), 3.56 (s, 1H, H-19), 3.80 (dd, 1H, *J₁* = 7.8 Hz, *J₂* = 1.0 Hz, H-28b), 6.98 (dd, 1H, *J₁* = 7.6 Hz, *J₂* = 4.7 Hz), 7.25 (d, 1H, *J* = 8.3 Hz), 8.46–8.44 (m, 1H, 3 × H–pyridine); ^{13}C NMR (126 MHz, CDCl₃) δ: 16.66, 15.58, 16.13, 20.30, 21.71, 24.20, 24.73, 26.40, 26.58, 26.65, 28.95, 28.98, 31.76, 32.87, 33.24, 34.46, 36.44, 36.89, 39.60, 40.63, 40.91, 41.66, 46.23, 46.95, 49.53, 53.81, 71.45, 88.07, 120.78, 129.70, 137.60, 147.41, 164.05; IR (DRIFT) *ν*max: 2942, 2859 cm⁻¹; HRMS (ESI⁺) *m/z* calcd for C₃₃H₅₀NO [M+H]⁺ 476.3886, found 476.3887.

4.3. General procedure for preparing 30-oxo derivatives (procedure B)

A modified literature procedure was used [26]. To a stirred solution of triterpenic acid **1b** or **9** in 2-methoxyethanol was added SeO₂ (2 equiv.) and the solution was refluxed. Reaction was monitored by TLC (toluene/diethyl ether 4 : 1) which indicated its completion after 4–6 h. Then the reaction mixture was filtered and diluted with water. The product was extracted with EtOAc (4 × 10 mL). The combined organic extracts were dried over MgSO₄ and concentrated under reduced pressure. The residue was purified by column chromatography on silica with Tol/Et₂O (from 10:1 to 2:1) as an eluent to give compounds **8** and **11**.

4.3.1. 30-Oxolupa-2,20(29)-dieno [2,3-b]pyridine-28-oic acid 8

SeO₂ (498 mg, 4.5 mmol, 2.2 equiv.) was added to a solution of pyrazine **1b** (1 g, 2.0 mmol) in 2-methoxyethanol (30 mL) and the re-action mixture was stirred under reflux for 6 h. Crude product was precipitated by pouring into cold water, filtered off, dried and chro-matographed on silica with Tol/Et₂O (from 5 : 1 to 2 : 1). Collected fractions were evaporated which yielded white solid of **8**. Yield: 565 mg (55%), white solid, m.p. 265–267 °C; ^{1}H NMR (500 MHz, CDCl₃) δ: 0.79 (s, 3H); 1.00 (s, 3H); 1.01 (s, 3H); 1.26 (s, 3H); 1.29 (s, 3H, 5 × CH₃); 1.74 (dd, 1H, *J₁* = 22.4 Hz, *J₂* = 10.9 Hz); 1.97–2.04 (m, 1H); 2.23–2.37 (m, 2H); 2.43 (d, 1H, *J* = 16.6 Hz, H-19β); 3.02 (d, 1H, *J* = 16.6 Hz); 3.37 (td, 1H, *J₁* = 11.2 Hz, *J₂* = 4.8 Hz, H-3α); 5.95 (s, 1H, H-29a); 6.31 (s, 1H, H-29b); 8.28 (d, 1H, *J* = 2.5 Hz), 8.42 (d, 1H, *J* = 1.8 Hz, 2 × H–pyrazine), 9.55 (s, 1H, H-30); ^{13}C NMR (126 MHz, CDCl₃) δ: 14.73, 14.81, 15.79, 16.24, 20.20, 21.54, 24.13, 27.32, 29.82, 31.63, 32.04, 32.15, 33.48, 36.93, 37.05, 38.53, 39.66, 40.67, 42.61, 48.67, 48.74, 50.45, 53.18, 56.65, 134.27, 141.47, 142.53, 150.81, 156.25, 159.91, 181.33, 195.17; IR (DRIFT) *ν*max: 2938, 2868, 1683, 1431 cm⁻¹; HRMS (ESI⁺): *m/z* calcd for C₃₂H₄₄N₂O₃ [M+H]⁺ 505.3425, found 505.3425.

4.3.2. 30-Oxolup-20(29)-en-28-oic acid 11

Compound **11** was prepared from betulinic acid **9** (1 g, 2.2 mmol) according to the general procedure. Yield: 505 mg (49%), white solid. Analytical and spectral data were in agreement with the literature [26].

4.4. General procedure for preparing propargyl esters (procedure C)

To a stirred solution of starting material in DMF was added potassium carbonate (K$_2$CO$_3$, 3 equiv.) and propargyl bromide (2 equiv.). The reaction mixture was stirred at room temperature and the progress of the reaction was monitored by TLC (Tol/Et$_2$O = 5 : 1, v/v), which indicated its completion after 4 h. The reaction mixture was filtered and diluted with water. The product was extracted with EtOAc (4 × 10 mL). The combined organic extracts were dried over MgSO$_4$ and concentrated under reduced pressure. The residue was purified by column chromatography on silica with Tol/Et$_2$O (from 20 : 1 to 2 : 1) as an eluent to give each propargyl ester.

4.4.1. Propargyl 3β-hydroxylup-20(29)-en-28-oate 10

Compound **10** was prepared according to the general procedure **C** with betulinic acid **9** (3 g, 6.6 mmol). Yield: 2.3 g (71%), white solid, m. p. 184–186 °C; ^{1}H NMR (500 MHz, CDCl$_3$) δ: 0.67–0.69 (m, 1H), 0.75 (s, 3H), 0.82 (s, 3H), 0.93 (s, 3H), 0.96 (s, 3H), 0.97 (s, 3H), 1.68 (s, 3H, 6 × CH$_3$), 1.84–1.96 (m, 2H), 2.16–2.24 (m, 1H), 2.25–2.31 (m, 1H), 2.35 (s, 1H), 2.43 (t, 1H, J = 2.4 Hz), 2.97–3.05 (m, 1H), 3.18 (dd, 1H, J$_1$ = 11.4 Hz, J$_2$ = 4.9 Hz), 4.60 (dd, 1H, J$_1$ = 2.2 Hz, J$_2$ = 1.4 Hz, H-29-pro E), 4.70 (dd, 1H, J$_1$ = 15.5 Hz, J$_2$ = 2.4 Hz, H-29-pro Z), 4.74 (d, 1H, J = 2.1 Hz), 7.12–7.19 (m, 1H); ^{13}C NMR (126 MHz, CDCl$_3$) δ: 14.86, 15.49, 16.17, 16.28, 18.45, 19.54, 25.70, 27.57, 28.13, 29.79, 30.68, 32.11, 34.50, 36.94, 37.36, 38.44, 38.89, 39.01, 40.97, 42.56, 47.01, 49.68, 50.74, 51.46, 55.53, 56.75, 74.46, 79.13, 109.79, 128.36, 129.17, 150.58, 175.32; IR (DRIFT) ν_{max}: 3273, 2938, 2869, 1720, 1642 cm^{-1}; HRMS (ESI$^+$): m/z calcd for C$_{33}$H$_{50}$O$_3$ [M+H]$^+$ 495.3883, found 495.3833.

4.4.2. Propargyl 3β-hydroxy-30-oxolup-20(29)-en-28-oate 12

Compound **12** was prepared according to the general procedure **C** with 30-oxo betulinic acid **11** (1 g, 1.97 mmol). Yield: 509 mg (47%), white solid: m.p. 188–192 °C; ^{1}H NMR (500 MHz, CDCl$_3$) δ: 0.74 (s, 3H), 0.80 (s, 3H), 0.90 (s, 3H), 0.92 (s, 3H), 0.95 (s, 3H, 5 × CH$_3$), 1.87–1.99 (m, 2H), 1.96–2.08 (m, 2H), 2.19 (td, 1H, J$_1$ = 12.5 Hz, J$_2$ = 3.6 Hz), 2.28–2.33 (m, 1H), 2.43 (t, 1H, J = 2.3 Hz), 3.16 (dd, 1H, J$_1$ = 11.3 Hz, J$_2$ = 4.8 Hz, H-19β), 3.33 (td, 1H, J$_1$ = 11.1 Hz, J$_2$ = 4.8 Hz, H-3α), 4.67 (dd, 1H, J$_1$ = 21.1 Hz, J$_2$ = 2.4 Hz), 5.89 (s, 1H, H - 29a), 6.27 (s, 1H, H-29b), 9.51 (s, 1H, H-30); ^{13}C NMR (126 MHz, CDCl$_3$) δ: 14.74, 15.49, 16.12, 16.23, 18.41, 20.99, 27.33, 27.52, 28.11, 29.70, 29.83, 31.87, 32.00, 34.44, 36.76, 37.30, 38.27, 38.86, 38.99, 40.88, 42.47, 50.51, 50.62, 51.53, 55.46, 56.82, 74.53, 77.16, 78.23, 79.08, 156.27, 175.14, 195.06; ν_{max}: 3558, 3294, 2946, 1730, 1671 cm^{-1}; HRMS (ESI$^+$): m/z calcd for C$_{33}$H$_{48}$O$_4$ [M+H]$^+$ 509.3628, found 509.3630.

4.4.3. Propargyl lupa-2,20(29)-dieno [2,3-b]pyridine-28-oate 13

Compound **13** was prepared according to the general procedure **C** with pyrazine **1b** (500 mg, 1 mmol). Yield: 450 mg (83%), white solid: m.p. 177–181 °C; ^{1}H NMR (500 MHz, CDCl$_3$) δ: 0.80 (s, 3H), 1.01 (s, 3H), 1.02 (s, 3H), 1.27 (s, 3H), 1.29 (s, 3H), 1.71 (s, 3H, 6x CH$_3$), 1.75–1.79 (m, 1H), 1.88–1.97 (m, 2H), 2.26–2.32 (m, 2H), 2.42–2.47 (m, 2H), 3.00–3.06 (m, 2H), 4.62–4.66 (m, 2H, H-29 *pro-E* and H-33a), 4.72 (dd, 1H, J$_1$ = 15.5 Hz, J$_2$ = 2.5 Hz, H-33b), 4.76 (d, 1H, J = 2.1 Hz, H-29 pro-Z), 8.26 (d, 1H, J = 2.4 Hz), 8.39 (dd, 1H, J$_1$ = 2.4 Hz, J$_2$ = 0.8 Hz, 2 × H–pyrazine); ^{13}C NMR (126 MHz, CDCl$_3$) δ: 14.85, 15.79, 16.26, 19.62, 20.25, 21.59, 24.16, 25.71, 29.80, 30.71, 31.65, 32.05, 33.53, 36.92, 36.97, 38.51, 39.64, 40.84, 42.63, 46.97, 48.89, 48.98, 49.59, 51.49, 53.24, 56.79, 74.47, 78.29, 109.91, 141.65, 142.41, 150.43, 151.01, 159.80, 175.31; IR (DRIFT) ν_{max}: 3279, 2937, 2874, 1716, 1744 cm^{-1}; HRMS (ESI$^+$): m/z calcd for C$_{35}$H$_{48}$N$_2$O$_2$ [M+H]$^+$ 529.3789, found 529.3787.

4.4.4. Propargyl 30-oxolupa-2,20(29)-dieno [2,3-b]pyridine-28-oate 14

Compound **14** was prepared according to the general procedure **C** with 30-oxo pyrazine **8** (300 mg, 0.6 mmol). Yield: 151 mg (47%), white solid, m.p. 200–204 °C; ^{1}H NMR (500 MHz, CDCl$_3$) δ: ^{1}H NMR δ: 0.78 (s,

3H), 0.98 (s, 3H), 0.99 (s, 3H), 1.26 (s, 3H), 1.28 (s, 3H, 5 × CH$_3$), 1.71 (dd, 1H, J$_1$ = 21.9 Hz, J$_2$ = 10.9 Hz), 1.93 (dd, 1H, J$_1$ = 12.5 Hz, J$_2$ = 7.9 Hz), 2.00–2.08 (m, 2H), 2.23–2.36 (m, 1H), 2.40–2.44 (m, 2H), 3.00 (d, 1H, J$_1$ = 16.5 Hz, J$_2$ = 4.8 Hz, H-19β), 3.35 (td, 1H, J$_1$ = 11.1 Hz, J$_2$ = 4.7 Hz, H-3α), 4.69 (dq, 1H, J$_1$ = 37.9 Hz, J$_2$ = 15.5 Hz, J$_3$ = 2.3 Hz), 5.93 (s, 1H, H-29a), 6.30 (s, 1H, H-29b), 8.25 (d, 1H, J = 2.3 Hz), 8.39 (d, 1H, J = 1.8 Hz, 2 × H–pyrazine), 9.54 (s, 1H, H-30); ^{13}C NMR (126 MHz, CDCl$_3$) δ: 14.73, 15.74, 16.22, 20.21, 21.53, 24.15, 25.90, 27.29, 29.71, 31.63, 31.81, 31.88, 33.46, 36.74, 36.91, 38.35, 39.63, 40.75, 42.55, 48.75, 48.80, 50.33, 51.56, 53.15, 56.85, 74.55, 78.23, 134.52, 141.58, 142.46, 150.88, 156.05, 159.82, 175.14, 195.13; IR (DRIFT) ν_{max}: 3273, 2931, 1735, 1681 cm^{-1}; HRMS (ESI$^+$): m/z calcd for C$_{35}$H$_{46}$N$_2$O$_3$ [M+H]$^+$ 543.3581, found 543.3582.

4.5. General procedure for preparing triterpenic glucose conjugates (procedure D)

To a stirred solution of triterpenic alkynes in DMF was added azide **II** or **III** (1.5 equiv.) and CuI (4 mol %, 0.016 mmol). The reaction mixture was stirred at 40 °C for 24 h. The reaction mixture was filtered and DMF was evaporated in vacuo. The crude products were dissolved in CH$_3$CN (3 mL) and purified by reverse phase HPLC (in gradient from 80% MeCN in H$_2$O to 100% CH$_3$CN) to afford final compounds **18–25**.

4.5.1. Conjugate 15

Compound **15** was prepared according to the general procedure **D** with alkyne **10** (0.3 g, 0.6 mmol) and azide **II**. Yield: 164 mg (31%), white solid, m.p. 120–122 °C; ^{1}H NMR (500 MHz, CDCl$_3$) δ: 0.73 (s, 3H); 0.79 (s, 3H), 0.80 (s, 3H), 0.93 (s, 3H), 0.94 (s, 3H, 5 × CH$_3$), 1.66 (s, 3H, 30-CH$_3$), 1.85 (s, 3H), 2.01 (s, 3H), 2.05 (s, 3H), 2.08 (s, 3H, 4 × Ac), 2.60 (s, 1H), 2.98 (td, 1H, J$_1$ = 11.0, J$_2$ = 4.5 Hz, H-19β), 3.16 (dd, 1H, J$_1$ = 11.3 Hz, J$_2$ = 4.8 Hz, H-3α), 3.99 (ddd, 1H, J$_1$ = 9.9 Hz, J$_2$ = 4.7 Hz, J$_3$ = 2.0 Hz), 4.12 (dd, 1H, J$_1$ = 12.6 Hz, J$_2$ = 1.9 Hz), 4.31 (dd, 1H, J$_1$ = 12.6 Hz, J$_2$ = 4.8 Hz), 4.58 (s, 1H, H-29 pro-E), 4.72 (s, 1H, H-29 pro-Z), 5.17–5.26 (m, 3H), 5.35–5.47 (m, 2H), 5.83–5.91 (m, 1H), 7.83 (s, 1H, triazole); ^{13}C NMR (126 MHz, CDCl$_3$) δ: 14.81, 15.47, 15.94, 16.25, 18.40, 19.43, 20.25, 20.64, 20.80, 20.99, 25.64, 27.51, 28.09, 29.74, 30.63, 32.06, 34.41, 36.98, 37.29, 38.37, 38.84, 38.97, 40.81, 41.10, 42.51, 47.02, 49.57, 50.66, 55.46, 56.67, 57.01, 61.59, 67.76, 70.44, 72.70, 75.37, 79.06, 85.94, 109.83, 122,16, 144.13, 150.54, 168.87, 169.44, 170.02, 170.57, 175.95; IR (DRIFT) ν_{max}: 3476, 1754, 1642 cm^{-1}; HRMS (ESI$^+$): m/z calcd for C$_{47}$H$_{69}$N$_3$O$_{12}$ [M+H]$^+$ 868.4954, found 868.4950.

4.5.2. Conjugate 16

Compound **16** was prepared according to the general procedure **D** with alkyne **10** (0.25 g, 0.5 mmol) and azide **III**. Yield: 163 mg (46%), white solid, m.p. 120–124 °C; ^{1}H NMR (500 MHz, CD$_3$OD) δ: 0.80 (s, 3H), 0.89 (s, 3H), 0.91 (s, 3H), 0.99 (s, 3H), 1.03 (s, 3H), 1.73 (s, 3H, 5 × CH$_3$), 2.29 (td, 2H, J$_1$ = 12.6 Hz, J$_2$ = 3.4 Hz), 3.02–3.10 (m, 1H), 3.17 (dd, 1H, J$_1$ = 11.4 Hz, J$_2$ = 4.8 Hz), 3.51–3.68 (m, 1H), 3.78 (dd, 1H, J$_1$ = 12.2 Hz, J$_2$ = 5.3 Hz), 3.89–3.97 (m, 2H), 4.64 (s, 1H, H-29 *pro-E*), 4.76 (d, 1H, J = 1.5 Hz, H-29 *pro-Z*), 5.26 (dd, 2H, J$_1$ = 32.0, J$_2$ = 12.8 Hz, glu-CH$_2$OH), 5.66 (d, 1H, J = 9.2 Hz), 8.26 (s, 1H, triazole); ^{13}C NMR (126 MHz, CD$_3$OD) δ: 15.11, 16.12, 16.62, 16.79, 19.45, 19.54, 22.06, 26.87, 28.04, 28.61, 30.79, 31.58, 32.96, 35.51, 37.77, 38.32, 39.61, 39.95, 40.09, 41.94, 43.52, 50.68, 51.99, 56.87, 57.68, 57.86, 62.41, 70.90, 73.53, 74.02, 78.53, 79.67, 81.18, 89.62, 110.31, 125.27, 144.17, 151.75, 177.08; IR (DRIFT) ν_{max}: 3353, 1725, 1665 cm^{-1}; HRMS (ESI$^+$): m/z calcd for C$_{39}$H$_{61}$N$_3$O$_8$ [M+H]$^+$ 700.4531, found 700.4528.

4.5.3. Conjugate 17

Compound **17** was prepared according to the general procedure **D** with alkyne **12** (0.21 g, 0.4 mmol) and azide **II**. Yield: 124 mg (33%), white solid, m.p. 159–163 °C; ^{1}H NMR (500 MHz, CDCl$_3$) δ: 0.74 (s, 3H),

0.78 (s, 3H), 0.80 (s, 3H), 0.91 (s, 3H), 0.95 (s, 3H, $5 \times CH_3$), 1.86 (s, 3H), 2.02 (s, 3H), 2.04 (s, 3H), 2.06 (s, 3H), 2.08 (s, 3H, $4 \times Ac$), 3.30–3.39 (m, 1H), 3.97–4.02 (m, 1H), 4.09–4.17 (m, 2H), 4.31 (dd, 1H, $J_1 = 12.6$ Hz, $J_2 = 5.0$ Hz), 5.23 (d, 2H, $J = 5.0$ Hz), 5.41–5.49 (m, 2H), 5.85–5.89 (m, 1H), 5.90 (s, 1H), 6.28 (s, 1H), 7.95 (s, 1H, triazole), 9.51 (d, 1H, $J = 10.7$ Hz, CHO); ^{13}C NMR (126 MHz, CDCl$_3$) δ: 14.34, 14.75, 15.48, 15.93, 16.21, 18.41, 20.27, 20.65, 20.67, 20.82, 20.99, 21.18, 27.43, 27.51, 28.11, 29.67, 29.83, 31.97, 34.41, 36.82, 37.29, 38.43, 38.86, 38.99, 40.77, 42.46, 50.48, 55.46, 56.80, 57.43, 60.53, 61.72, 67.84, 70.50, 72.78, 75.41, 79.08, 86.00, 122.19, 144.18, 156.39, 168.88, 169.47, 170.07, 170.60, 175.77, 195.08; IR (DRIFT) ν_{max}: 3557–3406, 1755, 1686, 1620 cm^{-1}; HRMS (ESI$^+$): m/z calcd for C$_{47}$H$_{67}$N$_3$O$_{13}$ [M+H]$^+$ 882.4747, found 882.4743.

4.5.4. Conjugate 18

Compound **18** was prepared according to the general procedure **D** with alkyne **12** (0.26 g, 0.51 mmol) and azide **III**. Yield: 190 mg (54%), white solid, m.p. 161–165 °C; ^{1}H NMR (500 MHz, CD$_3$OD) δ: 0.75 (s, 3H), 0.82 (s, 3H), 0.84 (s, 3H), 0.94 (s, 3H), 0.95 (s, 3H, $5 \times CH_3$), 3.11 (dd, 1H, $J_1 = 11.3$ Hz, $J_2 = 4.7$ Hz, 1H), 3.32–3.39 (m, 1H), 3.47–3.62 (m, 3H), 3.73 (dd, 1H, $J_1 = 12.2$ Hz, $J_2 = 5.2$ Hz), 3.84–3.93 (m, 2H), 5.23 (dd, 2H, $J_1 = 33.0$ Hz, $J_2 = 12.8$ Hz, glu-CH$_2$OH), 5.62 (d, 1H, $J = 9.2$ Hz), 6.03 (s, 1H, H-29 pro-E), 6.39 (s, 1H, H-29 pro-Z), 8.24 (s, 1H, triazole), 9.50 (s, 1H, CHO); ^{13}C NMR (126 MHz, CD$_3$OD) δ: 14.98, 16.11, 16.58, 16.74, 19.43, 22.07, 28.02, 28.60, 30.74, 32.74, 33.40, 35.50, 37.58, 38.29, 39.51, 39.94, 40.05, 40.44, 41.87, 43.42, 49.63, 51.80, 52.37, 56.83, 57.83, 57.96, 62.42, 70.90, 74.03, 78.52, 79.64, 81.18, 89.62, 125.26, 135.15, 144.17, 158.22, 176.92, 196.79; IR (DRIFT) ν_{max}: 3353, 1724, 1684 cm^{-1}; HRMS (ESI$^+$): m/z calcd for C$_{39}$H$_{59}$N$_3$O$_9$ [M+H]$^+$ 714.4324, found 714.4327.

4.5.5. Conjugate 19

Compound **19** was prepared according to the general procedure **D** with alkyne **13** (0.33 g, 0.6 mmol) and azide **II**. Yield: 170 mg (30%), white solid, m.p. 130–131 °C; ^{1}H NMR (500 MHz, CDCl$_3$) δ: 0.77–0.82 (m, 3H), 0.91 (s, 3H), 0.99 (s, 3H), 1.26–1.27 (m, 3H), 1.28 (s, 3H), 1.69 (s, 3H, $6 \times CH_3$), 1.85–1.87 (m, 3H), 2.02 (s, 3H), 2.04 (s, 3H), 2.06–2.08 (m, $4 \times Ac$), 2.22–2.31 (m, 2H), 2.43 (d, 1H, $J = 16.6$ Hz), 2.95–3.07 (2H, H-19β a H-1a), 4.16 (ddd, 1H, $J_1 = 37.7$ Hz, $J_2 = 12.6$ Hz, $J_3 = 2.1$ Hz), 4.24–4.35 (m, 1H), 4.62 (s, 1H), 4.75 (dd, 1H, $J_1 = 9.5$ Hz, $J_2 = 1.7$ Hz), 5.14–5.33 (m, 3H), 5.36–5.47 (m, 2H), 5.77–5.90 (m, 1H), 7.84 (s, 1H), 8.26 (d, 1H, $J = 2.3$ Hz), 8.39 (d, 1H, $J = 1.8$ Hz, $2 \times$ H–pyrazine); ^{13}C NMR (126 MHz, CDCl$_3$) δ: 14.80, 15.58, 15.82, 16.24, 19.52, 20.23, 20.26, 20.64, 20.81, 21.55, 24.16, 25.66, 29.77, 30.67, 31.63, 32.01, 33.46, 36.92, 36.97, 38.45, 39.61, 40.69, 42.61, 46.99, 48.85, 48.92, 49.50, 53.18, 56.73, 57.05, 61.59, 67.77, 70.44, 72.71, 75.39, 85.97, 109.97, 122.11, 141.64, 142.42, 144.15, 150.40, 150.95, 159.77, 168.87, 169.44, 170.02, 170.55, 175.93; IR (DRIFT) ν_{max}: 1755, 1642 cm^{-1}; HRMS (ESI$^+$): m/z calcd for C$_{49}$H$_{67}$N$_5$O$_{11}$ [M+H]$^+$ 902.4910, found 902.4908.

4.5.6. Conjugate 20

Compound **20** was prepared according to the general procedure **D** with alkyne **13** (0.5 g, 0.95 mmol) and azide **III**. Yield: 261 mg (38%), white solid, m.p. 132–136 °C; ^{1}H NMR (500 MHz, CDCl$_3$) δ: 0.78 (s, 3H), 0.90 (s, 3H), 0.98 (s, 3H), 1.25 (s, 3H), 1.27 (s, 3H), 1.67 (s, 3H, $6 \times CH_3$), 2.23 (d, 2H, $J = 9.6$ Hz), 2.43 (d, 1H, $J = 16.4$ Hz, H-1a), 2.88–3.12 (m, 2H), 3.60 (s, 1H), 3.75–3.98 (m, 4H, $4 \times$ H – glucose), 4.13 (s, 1H), 4.60 (s, 1H, H-29 pro-E), 4.72 (s, 1H, H-29 pro-Z), 5.14 (dd, 3H, $J_1 = 66.2$ Hz, $J_2 = 12.16$ Hz), 5.56 (d, 1H, $J = 7.0$ Hz), 7.90 (s, 1H, triazole), 8.25 (s, 1H), 8.39 (s, 1H, $2 \times$ H–pyrazine); ^{13}C NMR (126 MHz, CDCl$_3$) δ: 14.82, 15.65, 16.31, 19.48, 20.24, 21.58, 24.22, 25.63, 29.82, 30.65, 31.63, 32.03, 33.48, 36.92, 36.97, 38.44, 39.63, 40.69, 42.61, 47.03, 48.69, 48.90, 49.47, 53.16, 56.73, 57.02, 61.06, 68.88, 72.58, 79.02, 87.95, 110.17, 124.59, 137.95, 141.46, 142.52, 143.27, 150.23, 150.77, 159.86, 176.01; IR (DRIFT) ν_{max}: 3367, 1725, 1641 cm^{-1};

HRMS (ESI$^+$): m/z calcd for C$_{41}$H$_{59}$N$_5$O$_7$ [M+H]$^+$ 734.4487, found 734.4488.

4.5.7. Conjugate 21

Compound **21** was prepared according to the general procedure **D** with alkyne **14** (0.2 g, 0.37 mmol) and azide **ii**. Yield: 123 mg (35%), white solid, m.p. 158–162 °C; ^{1}H NMR (500 MHz, CDCl$_3$) δ: 0.76–0.80 (m, 3H), 0.88–0.97 (m, 6H), 1.26 (s, 3H), 1.28 (s, 3H, $5 \times CH_3$), 1.86 (s, 3H), 1.98–2.10 (m, 12H, $4 \times Ac$), 2.41 (d, 1H, $J = 16.5$ Hz), 2.99 (d, 1H, $J_1 = 16.5$ Hz), 3.31–3.39 (m, 1H), 3.97–4.03 (m, 1H), 4.17 (ddd, 1H, $J_1 = 30.2$ Hz, $J_2 = 12.6$ Hz, $J_3 = 2.1$ Hz), 4.30 (td, 1H, $J_1 = 12.6$ Hz, $J_2 = 4.9$ Hz), 5.18 (q, 1H, $J = 12.9$ Hz), 5.22–5.32 (m, 1H, H-29 pro-E), 5.36–5.53 (m, 1H, H-29 pro-Z), 5.84 (dd, 1H, $J_1 = 28.9$ Hz, $J_2 = 9.2$ Hz), 5.91–5.99 (m, 2H), 6.30 (d, 1H, $J = 7.9$ Hz), 8.25 (d, 1H, $J = 2.2$ Hz), 8.39 (s, 1H, $2 \times$ H–pyrazine), 9.54 (d, 1H, $J = 9.9$ Hz, CHO); ^{13}C NMR (126 MHz, CDCl$_3$) δ: 14.72, 15.55, 16.19, 20.20, 20.26, 20.65, 20.80, 21.52, 24.15, 27.38, 29.68, 29.82, 31.63, 31.89, 33.44, 36.78, 36.89, 38.28, 38.49, 39.62, 40.64, 42.55, 48.72, 48.79, 50.53, 53.16, 56.83, 57.44, 61.69, 67.83, 69.60, 70.49, 72.76, 75.40, 85.99, 122.15, 141.57, 142.47, 144.16, 148.07, 150.81, 156.17, 159.81, 168.87, 169.45, 170.05, 170.56, 175.74, 195.13; IR (DRIFT) ν_{max}: 3538–3402, 1754, 1689, 1621 cm^{-1}; HRMS (ESI$^+$): m/z calcd for C$_{49}$H$_{66}$N$_5$O$_{12}$ [M+H]$^+$ 916.4702, found 916.4701.

4.5.8. Conjugate 22

Compound **22** was prepared according to the general procedure **D** with alkyne **14** (0.3 g, 0.42 mmol) and azide **III**. Yield: 92 mg (29%), white solid, m.p. 152–158 °C; ^{1}H NMR (500 MHz, CD$_3$OD) δ: 0.81 (s, 3H), 0.90 (s, 3H), 1.01 (s, 3H), 1.29 (s, 3H), 1.29 (s, 3H, $5 \times CH_3$), 2.25–2.32 (m, 2H), 2.48 (d, 1H, $J = 16.6$ Hz), 2.97 (d, 1H, $J = 16.6$ Hz), 3.38 (td, 1H, $J_1 = 11.2$ Hz, $J_2 = 4.8$ Hz, H-19β), 3.48–3.61 (m, 2H), 3.72 (dd, 1H, $J_1 = 12.2$ Hz, $J_2 = 5.3$ Hz), 3.85–3.94 (m, 2H), 5.25 (dd, 2H, $J_1 = 37.7$ Hz, $J_2 = 12.8$ Hz), 5.62 (d, 1H, $J = 9.2$ Hz), 6.06 (s, 1H, H-29 pro-E), 6.42 (s, 1H, H-29 pro-Z), 8.23–8.27 (m, 2H, pyrazine and triazole), 8.44 (d, $J = 2.1$ Hz, 1H pyrazine), 9.52 (s, 1H, CHO); ^{13}C NMR (126 MHz, CD$_3$OD) δ: 14.94, 16.14, 16.64, 21.16, 22.65, 24.43, 28.58, 30.75, 31.76, 32.68, 34.44, 37.56, 37.81, 39.61, 40.60, 41.71, 43.53, 49.00, 49.79, 52.10, 54.16, 57.83, 57.99, 62.42, 70.90, 74.03, 78.53, 81.19, 89.62, 115.03, 125.30, 128.82, 135.35, 142.32, 143.83, 144.17, 151.97, 158.17, 161.35, 176.93, 196.83; IR (DRIFT) ν_{max}: 3348, 1723, 1686, 1620 cm^{-1}; HRMS (ESI$^+$): m/z calcd for C$_{41}$H$_{57}$N$_5$O$_8$ [M+H]$^+$ 748.4285, found 748.4280.

4.6. General procedure for preparing medoxomil derivatives (procedure E)

To a stirred solution of 4-(Chloromethyl)-5-methyl-1,3-dioxol-2-one (2.3 equiv.) in acetone (18 mL) triterpenic acid, KI (1.2 equiv.) and K$_2$CO$_3$ (3.3 equiv.) were added. The reaction mixture was stirred at room temperature and the progress of the reaction was monitored by TLC (Tol/EtOAc = 5 : 1, v/v), which indicated its completion after 24 h. Acetone was removed from reaction under reduced pressure and dissolved in EtOAc. The extract was washed sequentially with water and brine, product extracted with EtOAc (4×10 mL) and combined organic extracts were dried over MgSO$_4$ and concentrated under reduced pressure. The residue was purified by column chromatography on silica with Tol/Et$_2$O (from 20 : 1 to 2 : 1) as an eluent to give compounds **23–25**.

4.6.1. (5-Methyl-2-oxo-1,3-dioxol-4-yl)methyl 3β-hydroxylup-20(29)-en-28-oate 23

Compound **23** was prepared according to the general procedure **E** with betulinic acid **9** (228 mg, 0.5 mmol). Yield: 210 mg (74%), white solid, m.p. 213–216 °C; ^{1}H NMR (500 MHz, CDCl$_3$) δ: 0.75 (s, 3H), 0.81 (s, 3H), 0.83 (s, 3H), 0.94–0.97 (m, 6H, 5x CH$_3$), 1.16 (dt, 1H, $J_1 = 13.7$, $J_2 = 3.3$ Hz), 1.68 (s, 3H), 2.11 (td, 1H, $J_1 = 12.7$, $J_2 = 3.6$ Hz), 2.20 (s, 3H), 2.24 (dt, 1H, $J_1 = 13.0$, $J_2 = 3.3$ Hz), 2.92–2.99 (m, 1H, H-19β),

3.17 (dd, 1H, J_1 = 11.4, J_2 = 4.8 Hz, H-3α), 4.59–4.62 (m, 1H), 4.74 (d, 1H, *J* = 1.6 Hz), 4.76 (d, 1H, *J* = 13.8 Hz), 4.93 (d, 1H, *J* = 13.8 Hz); ^{13}C NMR (126 MHz, CDCl$_3$) *δ*: 9.59, 14.86, 15.48, 15.80, 16.27, 18.43, 19.52, 21.04, 25.65, 27.56, 28.13, 29.73, 30.68, 32.11, 34.45, 36.91, 37.35, 38.54, 38.87, 39.01, 40.78, 42.55, 47.07, 49.63, 50.67, 53.18, 55.51, 56.92, 79.13, 109.94, 134.15, 140.07, 150.33, 152.30, 175.66; IR (DRIFT) *ν*$_{max}$: 3557, 1816, 1735, 1641 cm^{-1}; HRMS (ESI$^-$): *m/z* calcd for C$_{35}$H$_{52}$O$_6$ [M+H]$^-$ 567.3680, found 567.3689.

4.6.2. (5-Methyl-2-oxo-1,3-dioxol-4-yl)methyl 3-oxolup-20(29)-en-28-oate 24

Compound **24** was prepared according to the general procedure **E** with betulonic acid **1a** (227 mg, 0.5 mmol). Yield: 225 mg (81%), white solid, m.p. 147–150 °C; ^{1}H NMR (500 MHz, CDCl$_3$) *δ*: 0.87 (s, 3H), 0.92 (s, 3H), 0.96 (s, 3H), 1.01 (s, 3H), 1.06 (s, 3H, 5 × CH$_3$), 1.18 (dt, 1H, J_1 = 13.7, J_2 = 3.4 Hz), 1.31 (d, 1H, *J* = 3.5 Hz), 1.62 (t, 1H, *J* = 11.4 Hz), 1.68 (s, 3H), 2.12–2.18 (m, 1H), 2.21 (s, 3H), 2.25 (dt, 1H, J_1 = 13.1, J_2 = 3.3 Hz), 2.34–2.42 (m, 1H), 2.44–2.53 (m, 1H), 2.93–3.00 (m, 1H, H-19β), 4.60–4.63 (m, 1H), 4.72–4.74 (m, 1H), 4.76 (d, 1H, *J* = 13.9 Hz), 4.94 (d, 1H, J_1 = 13.8 Hz); ^{13}C NMR (126 MHz, CDCl$_3$) *δ*: 9.60, 14.78, 15.57, 16.10, 19.51, 19.77, 21.16, 21.55, 25.64, 26.76, 29.69, 30.63, 32.03, 33.73, 34.27, 36.87, 37.05, 38.60, 39.75, 40.71, 42.59, 47.03, 47.48, 49.53, 50.00, 53.20, 55.11, 56.88, 77.16, 110.01, 134.13, 140.09, 150.24, 152.29, 175.63, 218.24; IR (DRIFT) *ν*$_{max}$: 1823, 1727, 1707, 1641 cm^{-1}; HRMS (ESI$^+$): *m/z* calcd for C$_{35}$H$_{50}$O$_6$ [M+H]$^+$ 567.3680, found 567.3683.

4.6.3. (5-Methyl-2-oxo-1,3-dioxol-4-yl)methyl lupa-2,20(29)-dieno [2,3-b]pyrazine-28-oate 25

Compound **25** was prepared according to the general procedure **E** with pyrazine **1b** (245 mg, 0.5 mmol). Yield: 289 mg (96%), white solid, m.p. 100–104 °C; ^{1}H NMR (500 MHz, CDCl$_3$) *δ*: 0.80 (s, 3H), 0.91 (s, 3H), 1.01 (s, 3H), 1.27 (s, 3H), 1.29 (s, 3H, 5 CH$_3$), 1.70 (s, 3H), 2.21 (s, 3H), 2.26 (dt, 1H, J_1 = 12.9, J_2 = 3.2 Hz), 2.44 (d, 1H, *J* = 16.5 Hz), 2.92–3.05 (m, 2H), 4.62–4.66 (m, 1H), 4.73–4.78 (m, 2H), 4.97 (d, 1H, *J* = 13.8 Hz), 8.26 (d, 1H, *J* = 2.4 Hz), 8.40 (d, 1H, *J* = 2.3 Hz, 2 × H–pyrazine); ^{13}C NMR (126 MHz, CDCl$_3$) *δ*: 9.62, 14.84, 15.37, 16.26, 19.59, 20.22, 21.57, 24.17, 25.63, 29.72, 30.67, 31.37, 31.64, 32.01, 33.45, 36.87, 36.94.38.56, 39.63, 40.62, 42.60, 47.00, 48.83, 48.88, 49.50, 53.19, 56.94, 110.06, 134.14, 140.12, 141.64, 142,45, 150.18, 150.94, 152.32, 159.81, 175.64; IR (DRIFT) *ν*$_{max}$: 1823, 1731, 1641, 768 cm^{-1}; HRMS (ESI$^+$): *m/z* calcd for C$_{37}$H$_{50}$N$_2$O$_5$ [M+H]$^+$ 603.3792, found 603.3794.

4.6.4. (5-Methyl-2-oxo-1,3-dioxol-4-yl)methyl lupa-2,20(29)-dieno [2,3-b]pyridine-28-oate 26

Compound **26** was prepared according to the general procedure **E** with pyridine **1c** (500 mg, 1.0 mmol). Yield: 500 mg (83%), white solid, m.p. 181–183 °C; ^{1}H NMR (500 MHz, CDCl$_3$) *δ*: 0.78 (s, 3H), 0.92 (s, 3H), 1.01 (s, 3H), 1.26 (s, 3H), 1.30 (s, 3H, 5 × CH$_3$), 1.70 (s, 3H), 2.21 (s, 3H), 2.26 (dt, 1H, J_1 = 12.8, J_2 = 3.2 Hz), 2.32 (d, 1H, *J* = 15.7 Hz), 2.72 (d, 1H, *J* = 15.7 Hz), 2.99 (td, 1H, J_1 = 10.8, J_2 = 4.7 Hz), 4.59–4.68 (m, 1H), 4.72–4.85 (m, 2H), 4.95 (d, 1H, *J* = 13.8 Hz), 6.97 (dd, 1H, J_1 = 7.6, J_2 = 4.7 Hz), 7.21 (d, 1H, *J* = 7.6 Hz), 8.45 (dd, 1H, J_1 = 4.6, J_2 = 1.0 Hz, 3 × H–pyridine); ^{13}C NMR (126 MHz, CDCl$_3$) *δ*: 9.60, 14.85, 15.47, 15.82, 19.54, 20.34, 21.65, 24.23, 25.78, 29.74, 30.66, 31.77, 32.07, 33.66, 36.36, 36.90, 38.69, 39.60, 40.68, 42.62, 46.09, 47.06, 49.03, 49.57, 53.21, 53.67, 56.95, 109.99, 120.75, 129.65, 134.15, 137.57, 140.08, 147.39, 150.34, 152.30, 164.04, 175.68; IR (DRIFT) *ν*$_{max}$: 1824, 1726, 1401, 770 cm^{-1}; HRMS (ESI$^+$): *m/z* calcd for C$_{38}$H$_{51}$NO$_5$ [M+H]$^+$ 602.3840, found 602.3853.

4.6.5. (5-Methyl-2-oxo-1,3-dioxol-4-yl)methyl lup-2-eno [2,3-b]pyrazine-28-oate 27

Compound **27** was prepared according to the general procedure **E** with pyrazine **2b** (500 mg, 1.0 mmol). Yield: 490 mg (81%), white solid,

m.p. 199–201 °C; ^{1}H NMR (500 MHz, CDCl$_3$) *δ*: 0.77 (d, 3H, *J* = 6.8 Hz), 0.81 (s, 3H), 0.88 (d, 3H, *J* = 6.8 Hz), 0.90 (s, 3H), 0.99 (s, 3H, 5 × CH$_3$), 1.28 (s, 3H), 1.30 (s, 3H), 2.20 (s, 3H), 2.46 (d, 1H. *J* = 16.5 Hz), 3.04 (d, 1H, *J* = 16.5 Hz), 4.75 (d, 1H, *J* = 13.8 Hz), 4.94 (d, 1H, *J* = 13.8 Hz), 8.27 (dd, 1H, J_1 = 3.9, J_2 = 2.3 Hz), 8.39–8.42 (m, 1H, 2 × H–pyrazine); ^{13}C NMR (126 MHz, CDCl$_3$) *δ*: 9.60, 14.77, 14.82, 15.41, 16.24, 20.24, 21.64, 22.91, 23.15, 24.18, 27.04, 29.75, 29.87, 31.66, 31.95, 33.58, 36.93, 37.28, 38.49, 39.66, 40.67, 42.79, 44.33, 48.71, 48.87, 49.07, 53.11, 53.21, 57.41, 134.24, 140.06, 141.65, 142.49, 150.91, 152.33, 159.87, 175.87; IR (DRIFT) *ν*$_{max}$: 1818, 1730, 1443, 770 cm^{-1}; HRMS (ESI$^+$): *m/z* calcd for C$_{37}$H$_{52}$N$_2$O$_5$ [M+H]$^+$ 605.3949, found 605.3972.

4.6.6. (5-Methyl-2-oxo-1,3-dioxol-4-yl)methyl lup-2-eno [2,3-b]pyridine-28-oate 28

Compound **28** was prepared according to the general procedure **E** with pyridine **2c** (500 mg, 1.0 mmol). Yield: 472 mg (77%), white solid, m.p. 222–224 °C; ^{1}H NMR (500 MHz, CDCl$_3$) *δ*: 0.77 (d, 3H, *J* = 6.8 Hz), 0.79 (s, 3H), 0.88 (d, 3H, *J* = 6.9 Hz), 0.91 (s, 3H), 0.99 (s, 3H, 5 × CH$_3$), 1.27 (s, 3H), 1.31 (s, 3H), 2.21 (s, 3H), 2.74 (d, 1H, *J* = 15.6 Hz), 4.77 (d, 1H, *J* = 13.8 Hz), 6.97 (dd, 1H, J_1 = 7.6, J_2 = 4.6 Hz), 7.24 (d, 1H, *J* = 7.9 Hz), 8.45 (dd, 1H, J_1 = 4.5, J_2 = 0.9 Hz, 3 × H–pyridine); ^{13}C NMR (126 MHz, CDCl$_3$) *δ*: 9.60, 14.78, 14.83, 15.49, 15.79, 20.35, 21.68, 22.91, 23.13, 24.25, 27.14, 29.75, 29.93, 31.78, 31.98, 33.74, 36.35, 37.28, 38.55, 39.60, 40.69, 42.79, 44.34, 46.05, 48.78, 49.08, 53.10, 53.65, 57.41, 120.75, 129.63, 134.23, 137.55, 140.04, 147.42, 152.33, 164.07, 175.90; IR (DRIFT) *ν*$_{max}$: 1819, 1730, 1574, 1442, 771 cm^{-1}; HRMS (ESI$^+$): *m/z* calcd for C$_{38}$H$_{53}$NO$_5$ [M+H]$^+$ 604.3997, found 604.4009.

4.7. Biological evaluation

4.7.1. Cell culture and MTS cytotoxicity assay

Cytotoxicity screening was done according to the routine protocol developed earlier at our department [48,49] All cells (if not indicated otherwise) were purchased from the American Tissue Culture Collection (ATCC). The CCRF-CEM line is derived from T lymphoblastic leukemia, evincing high chemosensitivity, K562 represent cells from an chronic myeloid leukemia patient sample with bcr-abl translocation, U2OS cell line is derived from osteosarcoma, HCT116 is colorectal tumor cell line and its p53 gene knock-down counterpart (HCT116p53−/−, Horizon Discovery Ltd, UK) is a model of human cancers with p53 mutation frequently associated with poor prognosis, A549 line is lung adenocarcinoma, HeLa cell line is cervix adenocarcinoma. The daunorubicin resistant subline of CCRF-CEM cells (CEM-DNR bulk) and paclitaxel resistant subline K562-TAX were selected in our laboratory by the long term cultivation of maternal cell lines in presence of increasing concentrations of daunorubicine or paclitaxel, respectively. The CEM-DNR bulk cells overexpress MRP-1 and P-glycoprotein, while K562-TAX cells overexpress P-glycoprotein only. Both proteins belong to the family of ABC transporters and are involved in the primary and/or acquired multidrug resistance phenomenon [50]. MRC-5 and BJ cell lines were used as a non-tumor control and represent human fibroblasts. The cells were maintained in nunc/corning 75 cm^2 plastic tissue culture flasks and cultured in appropriate cell culture medium according to the ATCC or Horizon recommendations (DMEM/RPMI 1640 with 5 g/L glucose, 2 mM glutamine, 100 U/mL penicillin, 100 mg/mL streptomycin, 10% fetal calf serum, and NaHCO$_3$). The cytotoxicity MTS assays were performed according to the standard procedure used at our institute and as described earlier [48,51,52].

4.7.2. Pharmacological parameters, chemical stability assay, stability in human plasma, microsomal stability assay, parallel artificial membrane permeability assay

These experiments were performed in the same way as in our earlier work [53] and according to the lit [34]. he detailed description is in the supporting information file.

4.7.3. Protein plasma binding

The assay is based on rapid equilibrium dialysis (RED) [54]. The plate inserts (Thermo Scientific™, Rockford, USA) for RED consist of two chambers (red and white) separated by a semi-permeable membrane. The 300 μL solution of each test compound (10 μM concentration) in 10% human plasma was transferred into the red chamber and white chamber was filled with 500 μL PBS buffer, pH 7.4. After the 4-h incubation, the equal volumes of the solutions from either compartment were transferred into the plate. 10% plasma or PBS buffer, pH 7.4 was added in order all the samples had the same matrix. The reactions were stopped by the addition of CH_3CN: methanol (2:1). Following centrifugation, the supernatants were lyophilized. The samples were dissolved in the mobile phase containing internal standard and are analyzed by the RF-MS.

4.7.4. Cell cultures

Cell cultures are fully described in the supporting information file.

4.7.5. Transport studies

MDR1-MCDK differentiated monolayers in Transwell® (96-well) plates [27] were used only if they were intact, as confirmed by Lucifer Yellow Rejection Assay. Prior to the experiment, the cells were washed twice with Hank's balanced buffer solution (HBBS) (Gibco, Waltham, USA) and pre-equilibrated for 1 h with HBSS buffered at pH 7.4. After removing the medium, the cells were treated with test compounds (at 10 μM in HBSS pH 7.4) for 1 h. After the incubation, the samples were lyophilized, dissolved in the mobile phase containing internal standard and analyzed on the RF-MS.

All experiments were done in duplicate. The apparent permeability coefficient was calculated as $P_{app} = (dQ/dt)/(C_0 \times A)$, where dQ/dt is the rate of permeation of the drug across the cell monolayer, C_0 is the donor compartment concentration at time t = 0 and A is the area of the cell monolayer. Efflux ratio R was defined as ratio P_{BA}/P_{AB} where P_{BA} and $/P_{AB}$ represent the apparent permeability of test compound from the basal to apical and apical to basal side of cell monolayer, respectively. The compounds with the efflux ratio of 2 or higher were considered as potential P-gp substrates.

4.7.6. Cell death evaluation using Annexin V

Cell death in CCRF-CEM cells was evaluated using Annexin V/propidium iodide combine staining. Cells were treated by **1b**, **8**, **21**, **22**, **23**, and **24** at $1 \times IC_{50}$ or $5 \times IC_{50}$ concentrations for 24 h. Then, cells harvested by centrifugation ($600 \times g$, 5 min, room temperature) were washed by ice-cold PBS and centrifuged again. The pellet was resuspended in annexin V binding buffer (10 mM HEPES/NaOH – pH 7.4, 140 mM NaCl, 2.5 mM $CaCl_2$) and density was adjusted to a final concentration of 5×10^5 cells per mL. The aliquot of 100 μL was stained by adding 5 μL of FITC conjugated Annexin V and 5 μL of propidium iodide solution (0.1 mg/mL). The samples were gently vortexed and incubated for 15 min at room temperature in the dark. Finally, cells were centrifuged, resuspended in 100 μL of annexin binding buffer and analyzed by FACSAria II (Becton Dickinson) flow cytometer. At least 10 000 cells per sample were acquired.

4.7.7. Western blot

CCRF-CEM cells were treated with derivatives **1b**, **8**, **21**, **22**, **23**, and **24** at $1 \times IC_{50}$ and $5 \times IC_{50}$ concentrations for 24 h. Cell pellets were washed with ice cold PBS and lysed in RIPA buffer (50 mM Tris-HCl pH 8.0, 150 mM NaCl, 1% NP-40, 0.5% sodium deoxycholate, 0.1% SDS, 1 mM EDTA and cOmplete™ Protease Inhibitor Cocktail (Roche)). Protein concentrations were determined using the Pierce™ BCA Protein Assay Kit (Thermo Scientific). In total, 10 μg of cellular proteins were denatured in Laemmli buffer (10% β-mercaptoethanol, 0.06% bromophenol blue, 47% glycerol, 12% SDS, 0.5 M Tris pH 6.8), separated by SDS-polyacrylamide gel electrophoresis, and transferred onto a nitrocellulose membrane using the Trans-Blot® Turbo™ Transfer System (Bio-Rad). The membranes were then incubated with primary antibodies against Bax (Cell Signaling Technology), Bid (Abcam), Bim (Cell Signaling Technology), caspase-3 (Cell Signaling Technology), caspase-7 (Cell Signaling Technology), c-Myc (Abcam), Noxa (Abcam), PARP (Cell Signaling Technology), and β-actin (Sigma Aldrich) overnight at 4 °C, followed by incubation with an appropriate peroxidase-linked secondary antibody (Sigma Aldrich). Chemiluminescence signals were visualized using the ChemiDoc MP Documentation system (Bio-Rad).

4.7.8. Fluorescence microscopy

CCRF-CEM cultured as suspension or HeLa cells cultured on coverslips (12 mm in diameter) in a Petri dish were incubated with or without 10 μM **1b** or **8** for 4 h. After incubation, cells were fixed with 2% formaldehyde (10 min, room temperature), washed, permeabilised with 0.2% Triton X-100 and washed again. Then, samples were incubated with the primary *anti*-MT-CO2 antibody (1:100, 30 min, room temperature, Abcam) diluted in $1 \times$ PBS followed by secondary antibody incubation (AlexaFluor 488 or DyLight 649 anti-mouse antibody, 1 : 100, 30 min, room temperature, Jackson ImmunoResearch) and DAPI (10 μM, ThermoFisher Scientific) diluted in 25 mM Tris-HCl, pH = 7.5 and 150 mM NaCl.

In the case of CCRF-CEM cells, cells were processed before antibody labelling as follows: 2 mL of cell suspension was transferred from the Petri dishes into 15-mL centrifuge tubes, 12 mL of $1 \times$ PBS was added, and cells were centrifuged 10 min at $150 \times g$. Supernatant was removed except for 1 mL, cells were resuspended, 14 mL of buffer was added, and cells were centrifuged 10 min at $150 \times g$. This step was repeated one more time. Supernatant was removed except for 1 mL, samples were put on ice and processed using the CytoTrap and wet centrifugation according to the lit [55]. Briefly, 0.5 mL of $1 \times$ PBS and 0.25 mL of cell suspension was added per one CytoTrap, and cells were centrifuged 10 min at $150 \times g$. Next, following solutions were gradually added to the samples, each addition was followed by centrifugation step: 1 mL of 2% formaldehyde (10 min at $150 \times g$), 1 mL of 150 mM NaCl (5 min at $150 \times g$), 1 mL of 20 mM $CuSO_4$ and 150 mM NaCl (10 min at $150 \times g$), 1 mL of 150 mM NaCl (5 min at $150 \times g$), 1 mL of 150 mM NaCl (5 min at $150 \times g$), 1 mL of 0.2% Triton X-100 (10 min at $150 \times g$), and 1 mL of $1 \times$ PBS (10 min at $150 \times g$). After centrifugation, samples were removed from the CytoTraps and the antibody staining was performed on the drops of solutions as described above.

When the click reaction detection was performed, cells were processed similarly as in the case of MT-CO2 detection with these modifications: cells were incubated in the secondary antibody solution (DyLight 649 anti-mouse) without DAPI addition. After short washing with the $1 \times$ PBS buffer, samples were post-fixed with 2% formaldehyde (10 min, room temperature), washed, and incubated in the click-reaction solution containing 5-FAM azide (30 min, room temperature [56]). Then, samples were washed with 25 mM Tris-HCl, pH = 7.5 and 150 mM NaCl and stained with DAPI (10 μM, 30 min, room temperature).

The samples were viewed using an Olympus IX83 microscope (UPLSAPO O objective 100×, NA 1.4). Images were taken by a Zyla camera (Andor) with a resolution of 2048 × 2048 or 1024 × 1024 pixels using CellSense Dimension acquisition software (Olympus).

4.7.9. Electron microscopy

CCRF-CEM cells were cultivated in corning 75 cm^2 plastic tissue culture flasks. The next day, 10 μM solution of **1b** was added to one culture flask, the second one serves as a control. After 4-h incubation, cells were washed with the $1 \times$ PBS buffer and fixed with 2.5% glutaraldehyde and 2% formaldehyde in 100 mM cacodylate buffer supplemented with 2 mM $CaCl_2$ (2 h, room temperature). After incubation, samples were washed with 100 mM cacodylate buffer supplemented with 2 mM $CaCl_2$, followed by incubation with 1% osmium tetroxide and 1.5% potassium ferrocyanide in deionized water (1 h, room temperature), washing in deionized water, and staining with 1% uranyl acetate

(1 h, room temperature). Subsequently, samples were washed again, scratched off by cell scraper, and centrifuged (14 000×*g*, 5 min, room temperature). Supernatant was removed, 200 μL of 10% gelatine warmed to 37–40 °C was added, cells were resuspended and centrifuged (14 000×*g*, 5 min, room temperature). The excess of gelatine was removed, samples were placed on ice for 10 min, and then, post-fixed with 2.5% glutaraldehyde and 2% formaldehyde in 0.2 M PIPES (overnight, 4 °C). The next day, samples were washed with deionized water and cut into small pieces (to < 1 mm^3). Samples were dehydrated in ethanol series (30%, 50%, 70%, and 90% – each 30 min; 100%–2 × 30 min) and propylene oxide (2 × 30 min), infiltrated in the mixture of propylene oxide and Epon (1 : 1, 60 min and 1 : 3, overnight, 4 °C). Finally, samples were incubated in Epon resin for 2 h, embedded in freshly prepared Epon resin and polymerised at 60 °C for 48 h. Ultrathin, 70-nm, epon sections were cut on Leica UltraCut microtome (Leica Microsystems) with a diamond knife (Diatome Ltd.). The sections were post-stained with 3% uranyl acetate and viewed using electron microscope Morgagni (at 80 kV; FEI Company, Eindhoven, The Netherlands) equipped with MegaView III camera.

4.7.9.1. Spheroid culture and drug screening. Spheroids of colorectal HCT116 and cervical HeLa cancer cell lines were established as described previously [57]. Six-day-old spheroids were treated with compounds at 0.1–10 μM concentrations for 3 days and imaged using a fully automated CellVoyager High-Content Imaging System (Model CV7000; Yokogawa Electric Corporation, Tokyo, Japan) described before [57]. Acquired images were analyzed using an in-house algorithm developed in MatLab R2013b (MathWorks, Inc., Natick, MA) [57]. The effect of the compound on spheroid size was calculated as a percentage of untreated controls post 3-day treatment, and data were analyzed using GraphPad Prism software (GraphPad Prism, San Diego, CA). Statistical differences were considered significant at p < 0.05. All drug treatments were done in triplicates, and the experiments were repeated at 3 independent times [58].

Declaration of competing interest

The authors declare that they have no known competing financial interests or personal relationships that could have appeared to influence the work reported in this paper.

Data availability

Data will be made available on request.

Acknowledgment

Appendix A. Supplementary data

Supplementary data to this article can be found online at https://doi.org/10.1016/j.ejmech.2022.114777.

References

[1] L.F. Rocha e Silva, C. Ramalhete, K.L. Nogueira, S. Mulhovo, M.-J.U. Ferreira, A. M. Pohlit, In vivo evaluation of isolated triterpenes and semi-synthetic derivatives as antimalarial agents, Eur. J. Med. Chem. 102 (2015) 398–402, https://doi.org/10.1016/j.ejmech.2015.08.022.

[2] M.C. Sousa, R. Varandas, R.C. Santos, M. Santos-Rosa, V. Alves, J.A.R. Salvador, Antileishmanial activity of semisynthetic lupane triterpenoids betulin and betulinic acid derivatives: synergistic effects with miltefosine, PLoS One 9 (2014), https://doi.org/10.1371/journal.pone.0089939.

[3] C. Aiken, C.H. Chen, Betulinic acid derivatives as HIV-1 antivirals, Trends Mol. Med. 11 (2005) 31–36, https://doi.org/10.1016/j.molmed.2004.11.001.

[4] B. Bednarczyk-Cwynar, N. Wachowiak, M. Szulc, E. Kamińska, A. Bogacz, J. Bartkowiak-Wieczorek, L. Zaprutko, P.L. Mikolajczak, Strong and long-lasting antinociceptive and anti-inflammatory conjugate of naturally occurring oleanolic acid and aspirin, Front. Pharmacol. 7 (2016), https://doi.org/10.3389/fphar.2016.00202.

[5] P. Dzubak, M. Hajduch, D. Vydra, A. Hustova, M. Kvasnica, D. Biedermann, L. Markova, M. Urban, J. Sarek, Pharmacological activities of natural triterpenoids and their therapeutic implications, Nat. Prod. Rep. 23 (2006) 394–411, https://doi.org/10.1039/B515312N.

[6] L. Heller, A. Obernauer, R. Csuk, Simple structural modifications confer cytotoxicity to allobetulin, Bioorg. Med. Chem. 23 (2015) 3002–3012, https://doi.org/10.1016/j.bmc.2015.05.015.

[7] M. Kvasnica, M. Urban, N.J. Dickinson, J. Sarek, Pentacyclic triterpenoids with nitrogen- and sulfur-containing heterocycles: synthesis and medicinal significance, Nat. Prod. Rep. 32 (2015) 1303–1330, https://doi.org/10.1039/C5NP00015G.

[8] M. Urban, J. Sarek, M. Kvasnica, I. Tislerova, M. Hajduch, Triterpenoid pyrazines and benzopyrazines with cytotoxic activity, J. Nat. Prod. 70 (2007) 526–532, https://doi.org/10.1021/np060436d.

[9] R. Haavikko, A. Nasereddin, N. Sacerdoti-Sierra, D. Kopelyanskiy, S. Alakurtti, M. Tikka, C.L. Jaffe, J. Yli-Kauhaluoma, Heterocycle-fused lupane triterpenoids inhibit Leishmania donovani amastigotes, Med. Commun. 5 (2014) 445–451, https://doi.org/10.1039/C3MD00282A.

[10] J. Pokorny, L. Borkova, M. Urban, Click reactions in chemistry of triterpenes - advances towards development of potential therapeutics, Curr. Med. Chem. 25 (2018) 636–658, https://doi.org/10.2174/0929867324666171009122612.

[11] M. Urban, M. Vlk, P. Dzubak, M. Hajduch, J. Sarek, Cytotoxic heterocyclic triterpenoids derived from betulin and betulinic acid, Bioorg. Med. Chem. 20 (2012) 3666–3674, https://doi.org/10.1016/j.bmc.2012.03.066.

[12] M. Soural, J. Hodon, N.J. Dickinson, V. Sidova, S. Gurska, P. Dzubak, M. Hajduch, J. Sarek, M. Urban, Preparation of conjugates of cytotoxic lupane triterpenes with biotin, Bioconjugate Chem. 26 (2015) 2563–2570, https://doi.org/10.1021/acs.bioconjchem.5b00567.

[13] M. Laavola, R. Haavikko, M. Hämäläinen, T. Leppänen, R. Nieminen, S. Alakurtti, V.M. Moreira, J. Yli-Kauhaluoma, E. Moilanen, Betulin derivatives effectively suppress inflammation in vitro and in vivo, J. Nat. Prod. 79 (2016) 274–280, https://doi.org/10.1021/acs.jnatprod.5b00709.

[14] R. Haavikko, Synthesis of Betulin Derivatives with New Bioactivities, 2015. https://helda.helsinki.fi/bitstream/handle/10138/157276/synthesi.pdf?sequence=1.

[15] I.C. Sun, H.K. Wang, Y. Kashiwada, J.K. Shen, L.M. Cosentino, C.H. Chen, L. M. Yang, K.H. Lee, Anti-AIDS agents. 34. Synthesis and structure-activity relationships of betulin derivatives as anti-HIV agents, J. Med. Chem. 41 (1998) 4648–4657, https://doi.org/10.1021/jm980391g.

[16] L. Borkova, L. Jasikova, J. Rehulka, K. Frisonsova, M. Urban, I. Frydrych, I. Popa, M. Hajduch, N.J. Dickinson, M. Vlk, P. Dzubak, J. Sarek, Synthesis of cytotoxic 2,2-difluoroderivatives of dihydrobetulinic acid and allobetulin and study of their impact on cancer cells, Eur. J. Med. Chem. 96 (2015) 482–490, https://doi.org/10.1016/j.ejmech.2015.03.068.

[17] M. Urban, J. Sarek, I. Tislerova, P. Dzubak, M. Hajduch, Influence of esterification and modification of A-ring in a group of lupane acids on their cytotoxicity, Bioorg. Med. Chem. 13 (2005) 5527–5535, https://doi.org/10.1016/j.bmc.2005.07.011.

[18] M. Urban, M. Kvasnica, N.J. Dickinson, J. Sarek, Biologically active triterpenoids useable as prodrugs, in: A.R. Bates (Ed.), Terpenoids and Squalene: Biosynthesis, Functions and Health Implications, Nova Science Publishers, New York, 2015. https://www.novapublishers.com/catalog/product_info.php?products_id=52916&osCsid=bcdf867f385e9f4704bf0d72cae76d60. accessed September 13, 2016.

[19] M. Vlk, P. Micolova, M. Urban, M. Kvasnica, D. Saman, J. Sarek, 15N-labelled pyrazines of triterpenic acids, J. Radioanal. Nucl. Chem. 308 (2015) 733–739, https://doi.org/10.1007/s10967-015-4479-5.

[20] J. Pokorný, D. Olejníková, I. Frydrych, B. Lišková, S. Gurská, S. Benická, J. Šarek, J. Kotulová, M. Hajdúch, P. Džubák, M. Urban, Substituted dienes prepared from betulinic acid – synthesis, cytotoxicity, mechanism of action, and pharmacological parameters, Eur. J. Med. Chem. (2021), 113706, https://doi.org/10.1016/j.ejmech.2021.113706.

[21] P. Perlikova, M. Kvasnica, M. Urban, M. Hajduch, J. Sarek, 2-Deoxyglycoside conjugates of lupane triterpenoids with high cytotoxic activity—synthesis, activity, and pharmacokinetic profile, Bioconjugate Chem. 30 (2019) 2844–2858, https://doi.org/10.1021/acs.bioconjchem.9b00565.

[22] Y. Yoon, J.W. Lim, J. Kim, Y. Kim, K.H. Chun, Discovery of ursolic acid prodrug (NX-201): pharmacokinetics and in vivo antitumor effects in PANC-1 pancreatic cancer, Bioorg. Med. Chem. Lett 26 (2016) 5524–5527, https://doi.org/10.1016/j.bmcl.2016.10.008.

[23] A.P. Esteves, L.M. Rodrigues, M.E. Silva, S. Gupta, A.M.F. Oliveira-Campos, O. Machalicky, A.J. Mendonça, Synthesis and characterization of novel fluorescent N-glycoconjugates, Tetrahedron 61 (2005) 8625–8632, https://doi.org/10.1016/j.tet.2005.07.006.

[24] D. Bhunia, P.M.C. Pallavi, S.R. Bonam, S.A. Reddy, Y. Verma, M.S.K. Halmuthur, Design, synthesis, and evaluation of novel 1,2,3-triazole-tethered glycolipids as vaccine adjuvants, Arch. Pharmazie 348 (2015) 689–703, https://doi.org/10.1002/ardp.201500143.

[25] V. Sidova, P. Zoufaly, J. Pokorny, P. Dzubak, M. Hajduch, I. Popa, M. Urban, Cytotoxic conjugates of betulinic acid and substituted triazoles prepared by Huisgen Cycloaddition from 30-azidoderivatives, PLoS One 12 (2017), e0171621, https://doi.org/10.1371/journal.pone.0171621.

[26] M. Urban, J. Klinot, I. Tislerova, D. Biedermann, M. Hajduch, I. Cisarova, J. Sarek, Reactions of activated lupane oxo-compounds with diazomethane: an approach to new derivatives of cytotoxic triterpenes, Synthesis 2006 (2006) 3979–3986, https://doi.org/10.1055/s-2006-950327.

[27] J.D. Irvine, L. Takahashi, K. Lockhart, J. Cheong, J.W. Tolan, H.E. Selick, J. R. Grove, MDCK (Madin-Darby canine kidney) cells: a tool for membrane permeability screening, J. Pharmaceut. Sci. 88 (1999) 28–33, https://doi.org/10.1021/js9803205.

[28] A.F. Nassar, Structural modifications of drug candidates: how useful are they in improving metabolic stability of new drugs? Part I: enhancing metabolic stability, in: Drug Metabolism Handbook, John Wiley & Sons, Ltd, 2008, pp. 253–268, https://doi.org/10.1002/9780470439265.ch10.

[29] F. Wohnsland, B. Faller, High-Throughput permeability pH profile and high-throughput alkane/water log P with artificial membranes, J. Med. Chem. 44 (2001) 923–930, https://doi.org/10.1021/jm001020e.

[30] M.C. Wei, W.-X. Zong, E.H.-Y. Cheng, T. Lindsten, V. Panoutsakopoulou, A.J. Ross, K.A. Roth, G.R. MacGregor, C.B. Thompson, S.J. Korsmeyer, B.A.X. Proapoptotic, BAK, A requisite gateway to mitochondrial dysfunction and death, Science 292 (2001) 727–730, https://doi.org/10.1126/science.1059108.

[31] H. Zou, Y. Li, X. Liu, X. Wang, An APAF-1·Cytochrome c multimeric complex is a functional apoptosome that activates procaspase-9, J. Biol. Chem. 274 (1999) 11549–11556, https://doi.org/10.1074/jbc.274.17.11549.

[32] X. Cao, X. Deng, W.S. May, Cleavage of Bax to p18 Bax accelerates stress-induced apoptosis, and a cathepsin-like protease may rapidly degrade p18 Bax, Blood 102 (2003) 2605–2614, https://doi.org/10.1182/blood-2003-01-0211.

[33] S.J. Korsmeyer, M.C. Wei, M. Saito, S. Weiler, K.J. Oh, P.H. Schlesinger, Pro-apoptotic cascade activates BID, which oligomerizes BAK or BAX into pores that result in the release of cytochrome c, Cell Death Differ. 7 (2000) 1166–1173, https://doi.org/10.1038/sj.cdd.4400783.

[34] M.S. Satoh, T. Lindahl, Role of poly(ADP-ribose) formation in DNA repair, Nature 356 (1992) 356–358, https://doi.org/10.1038/356356a0.

[35] Y.A. Lazebnik, S.H. Kaufmann, S. Desnoyers, G.G. Poirier, W.C. Earnshaw, Cleavage of poly(ADP-ribose) polymerase by a proteinase with properties like ICE, Nature 371 (1994) 346–347, https://doi.org/10.1038/371346a0.

[36] M. Tewari, L.T. Quan, K. O'Rourke, S. Desnoyers, Z. Zeng, D.R. Beidler, G. G. Poirier, G.S. Salvesen, V.M. Dixit, Yama/CPP32β, a mammalian homolog of CED-3, is a CrmA-inhibitable protease that cleaves the death substrate poly(ADP-ribose) polymerase, Cell 81 (1995) 801–809, https://doi.org/10.1016/0092-8674(95)90541-3.

[37] P. Bouillet, A. Strasser, BH3-only proteins — evolutionarily conserved proapoptotic Bcl-2 family members essential for initiating programmed cell death, J. Cell Sci. 115 (2002) 1567–1574, https://doi.org/10.1242/jcs.115.8.1567.

[38] C. Ploner, R. Kofler, A. Villunger, Noxa: at the tip of the balance between life and death, Oncogene 27 (2008), https://doi.org/10.1038/onc.2009.46. S84–S92.

[39] E. Oda, R. Ohki, H. Murasawa, J. Nemoto, T. Shibue, T. Yamashita, T. Tokino, T. Taniguchi, † Nobuyuki Tanaka, Noxa, a BH3-only member of the bcl-2 family and candidate mediator of p53-induced apoptosis, Science 288 (2000) 1053–1058, https://doi.org/10.1126/science.288.5468.1053.

[40] Liam O'Connor, Bim: a novel member of the Bcl-2 family that promotes apoptosis, EMBO J. 17 (1998) 384–395, https://doi.org/10.1093/emboj/17.2.384.

[41] M. Henriksson, B. Lüscher, Proteins of the myc network: essential regulators of cell growth and differentiation, in: G.F. Vande Woude, G. Klein (Eds.), Advances in Cancer Research, Academic Press, 1996, pp. 109–182, https://doi.org/10.1016/S0065-230X(08)60353-X.

[42] A. Ligasová, M. Vydržalová, R. Buriánová, L. Brůčková, R. Večeřová, A. Janošťáková, K. Koberna, A new sensitive method for the detection of mycoplasmas using fluorescence microscopy, Cells 8 (2019) 1510, https://doi.org/10.3390/cells8121510.

[43] G. Monteuuis, A. Miścicka, M. Świrski, L. Zenad, O. Niemitalo, L. Wrobel, J. Alam, A. Chacinska, A.J. Kastaniotis, J. Kufel, Non-canonical translation initiation in yeast generates a cryptic pool of mitochondrial proteins, Nucleic Acids Res. 47 (2019) 5777–5791, https://doi.org/10.1093/nar/gkz301.

[44] V. Das, F. Bruzzese, P. Konečný, F. Iannelli, A. Budillon, M. Hajdúch, Pathophysiologically relevant in vitro tumor models for drug screening, Drug Discov. Today 20 (2015) 848–855, https://doi.org/10.1016/j.drudis.2015.04.004.

[45] W. Jiang, X. Li, S. Dong, W. Zhou, Betulinic acid in the treatment of tumour diseases: application and research progress, Biomed. Pharmacother. 142 (2021), 111990, https://doi.org/10.1016/j.biopha.2021.111990.

[46] H.I. Ciftci, M.O. Radwan, B. Sever, A.K. Hamdy, S. Emirdağ, N.G. Ulusoy, E. Sozer, M. Can, N. Yayli, N. Araki, H. Tateishi, M. Otsuka, M. Fujita, M.D. Altintop, EGFR-targeted pentacyclic triterpene analogues for glioma therapy, Int. J. Mol. Sci. 22 (2021), 10945, https://doi.org/10.3390/ijms222010945.

[47] O. Troitskaya, D. Novak, A. Nushtaeva, M. Savinkova, M. Varlamov, M. Ermakov, V. Richter, O. Koval, EGFR transgene stimulates spontaneous formation of MCF7 breast cancer cells spheroids with partly loss of HER3 receptor, Int. J. Mol. Sci. 22 (2021), 12937, https://doi.org/10.3390/ijms222312937.

[48] L. Borkova, R. Adamek, P. Kalina, P. Drašar, P. Dzubak, S. Gurska, J. Rehulka, M. Hajduch, M. Urban, J. Sarek, Synthesis and cytotoxic activity of triterpenoid thiazoles derived from allobetulin, methyl betulonate, methyl oleanonate, and oleanonic acid, ChemMedChem 12 (2017) 390–398, https://doi.org/10.1002/cmdc.201600626.

[49] L. Borkova, S. Gurska, P. Dzubak, R. Burianova, M. Hajduch, J. Sarek, I. Popa, M. Urban, Lupane and 18α-oleanane derivatives substituted in the position 2, their cytotoxicity and influence on cancer cells, Eur. J. Med. Chem. 121 (2016) 120–131, https://doi.org/10.1016/j.ejmech.2016.05.029.

[50] V. Noskova, P. Dzubak, G. Kuzmina, A. Ludkova, D. Stehlik, R. Trojanec, A. Janostakova, G. Korinkova, V. Mihal, M. Hajduch, In vitro chemoresistance profile and expression/function of MDR associated proteins in resistant cell lines derived from CCRF-CEM, K562, A549 and MDA MB 231 parental cells, Neoplasma 49 (2002) 418–425.

[51] A. Bourderioux, P. Nauš, P. Perlíková, R. Pohl, I. Pichová, I. Votruba, P. Džubák, P. Konečný, M. Hajdúch, K.M. Stray, T. Wang, A.S. Ray, J.Y. Feng, G. Birkus, T. Cihlar, M. Hocek, Synthesis and significant cytostatic activity of 7-Hetaryl-7-deazaadenosines, J. Med. Chem. 54 (2011) 5498–5507, https://doi.org/10.1021/jm2005173.

[52] B. Eignerova, M. Tichy, J. Krasulova, M. Kvasnica, L. Rarova, R. Christova, M. Urban, B. Bednarczyk-Cwynar, M. Hajduch, J. Sarek, Synthesis and antiproliferative properties of new hydrophilic esters of triterpenic acids, Eur. J. Med. Chem. 140 (2017) 403–420, https://doi.org/10.1016/j.ejmech.2017.09.041.

[53] L. Borková, I. Frydrych, N. Jakubcová, R. Adámek, B. Lišková, S. Gurská, M. Medvedíková, M. Hajdúch, M. Urban, Synthesis and biological evaluation of triterpenoid thiazoles derived from betulonic acid, dihydrobetulonic acid, and ursonic acid, Eur. J. Med. Chem. 185 (2020), 111806, https://doi.org/10.1016/j.ejmech.2019.111806.

[54] X. Wu, J. Wang, L. Tan, J. Bui, E. Gjerstad, K. McMillan, W. Zhang, In vitro ADME profiling using high-throughput rapidfire mass spectrometry: cytochrome p450 inhibition and metabolic stability assays, J. Biomol. Screen 17 (2012) 761–772, https://doi.org/10.1177/1087057112441013.

[55] J.K. Singh, A. Solanki, R.C. Maniyar, D. Banerjee, V.S. Shirsath, Rapid equilibrium dialysis (RED): an in-vitro high-throughput screening technique for plasma protein binding using human and rat plasma, J. Bioequivalence Bioavailab. (2012), https://doi.org/10.4172/jbb.S14-005.

[56] A. Ligasová, K. Koberna, New concept and apparatus for cytocentrifugation and cell processing for microscopy analysis, Int. J. Mol. Sci. 22 (2021) 7098, https://doi.org/10.3390/ijms22137098.

[57] A. Ligasová, K. Koberna, DNA replication: from radioisotopes to click chemistry, Molecules 23 (2018) 3007, https://doi.org/10.3390/molecules23113007.

[58] V. Das, T. Fürst, S. Gurská, P. Džubák, M. Hajdúch, Reproducibility of uniform spheroid formation in 384-well plates: the effect of medium evaporation, J. Biomol. Screen 21 (2016) 923–930, https://doi.org/10.1177/1087057116651867.